Quaternary Science Reviews 155 (2017) 159–178

Contents lists available at ScienceDirect

Quaternary Science Reviews

journal homepage: www.elsevier.com/locate/quascirev

Holocene climatic variations in the Western Cordillera of Colombia: A multiproxy high-resolution record unravels the dual influence of ENSO and ITCZ

Paula Muñoz [a, 1], Georges Gorin [a, *], Norberto Parra [b], Cesar Velásquez [b], Diego Lemus [c], Carlos Monsalve-M. [b], Marcela Jojoa [b, 2]

[a] Department of Earth Sciences, Earth and Environmental Science Section, University of Geneva, Rue des Maraîchers 13, CH-1205 Geneva, Switzerland
[b] Facultad de Ciencias, Universidad Nacional de Colombia, Sede Medellin, Calle 59A, No. 63-20, Medellin, Colombia
[c] Facultad de Estadística, Universidad Santo Tomás, Carrera 9, No. 51-11, Bogotá, Colombia

ARTICLE INFO

Article history:
Received 13 May 2016
Received in revised form
14 November 2016
Accepted 15 November 2016
Available online 24 November 2016

Keywords:
Humidity
Iron
Palaeoenvironmemt
Pollen
Rainfall
Temperature
Titanium
Wavelet analysis
X-ray fluorescence
Younger Dryas

ABSTRACT

The Páramo de Frontino (3460 m elevation) in Colombia is located approximately halfway between the Pacific and Atlantic oceans. It contains a 17 kyr long, stratigraphically continuous sedimentary sequence dated by 30 AMS 14C ages. Our study covers the last 11,500 cal yr and focuses on the biotic (pollen) and abiotic (microfluorescence-X or µXRF) components of this high mountain ecosystem. The pollen record provides a proxy for temperature and humidity with a resolution of 20–35 yr, and µXRF of Ti and Fe is a proxy for rainfall with a sub-annual (ca. 6-month) resolution.

Temperature and humidity display rapid and significant changes over the Holocene. The rapid transition from a cold (mean annual temperature (MAT) 3.5 °C lower than today) and wet Younger Dryas to a warm and dry early Holocene is dated at 11,410 cal yr BP. During the Holocene, MAT varied from ca. 2.5 °C below to 3.5° above present-day temperature. Warm periods (11,410–10,700, 9700–6900, 4000–2400 cal yr BP) were separated by colder intervals. The last 2.4 kyr of the record is affected by human impact. The Holocene remained dry until 7500 cal yr BP. Then, precipitations increased to reach a maximum between 5000 and 4500 cal yr BP. A rapid decrease occurred until 3500 cal yr BP and the late Holocene was dry. Spectral analysis of µXRF data show rainfall cyclicity at millennial scale throughout the Holocene, and at centennial down to ENSO scale in more specific time intervals. The highest rainfall intervals correlate with the highest activity of ENSO. Variability in solar output is possibly the main cause for this millennial to decadal cyclicity. We interpret ENSO and ITCZ as the main climate change-driving mechanisms in Frontino. Comparison with high-resolution XRF data from the Caribbean Cariaco Basin (a proxy for rainfall in the coastal Venezuelian cordilleras) demonstrates that climate in Frontino was Pacific-driven (ENSO-dominated) during the YD and early Holocene, whereas it was Atlantic-driven in Cariaco (ITCZ-dominated). From ca. 8000 cal yr BP, climate in both areas was under the dual influence of ENSO and ITCZ, thereby showing existing teleconnections between the tropical Pacific and Atlantic oceans.

The Frontino record is to date the highest-resolution Holocene study in NW Colombia. An implication of these results is that new records should be analyzed with multiproxy tools, in particular those providing high resolution time series, such as µXRF.

1. Introduction

Records of climate change are particularly important in the tropics, where major thermal energy interchanges take place between oceans and atmosphere. Climatic events like the migration of the Intertropical Convergence Zone (ITCZ, e.g., Haug et al., 2001, 2003; Petersen and Haug, 2006; Yancheva et al., 2007; Wanner

* Corresponding author.
E-mail address: georges.gorin@unige.ch (G. Gorin).
[1] Present address: Chalice Court Flat 1, 41 Chevening Rd, SE19 3TD Upper Norwood, UK.
[2] Present address: Universidad de Medellín, Carrera 87 N° 30–65, Medellín, Colombia.

http://dx.doi.org/10.1016/j.quascirev.2016.11.021

et al., 2008) and the El Niño-Southern Oscillation (ENSO, e.g., Thompson, 2000; Moy et al., 2002; Riedinger et al., 2002; Flantua et al., 2016a) are typically associated with the tropics but influence the global climate. The here studied high-altitude site, the Páramo de Frontino at the northern termination of the Colombian Western Cordillera (Fig. 1), is ideally located because it is exposed to the climatic influence of both the Atlantic and Pacific oceans.

In the last 50 years, Colombia has been one of the best-studied tropical countries with respect to Quaternary climate change and associated variations in the distribution of vegetation (Flantua et al., 2015). Palynology has been the main tool for these investigations: Van der Hammen and González (1960a,b), González et al. (1965), Van der Hammen et al. (1973), Van Geel and Van der Hammen (1973), Van der Hammen et al. (1980/1981), Hooghiemstra (1984), Kuhry (1988), Mommersteeg (1998), Thouret et al. (1996), Wille et al. (2001), Van der Hammen and Hooghiemstra (2003), Groot et al. (2011), among others. The period since the last glacial maximum is the best covered by pollen-based records from a variety of biomes (páramo, montane forest, savana, rainforest, dry forest), which were used to unravel the dynamic history of these ecosystems (e.g., Marchant et al., 2001, 2002, 2006; Flantua et al., 2015). In montane areas, the Eastern Cordillera of Colombia is palaeoecologically best studied, whereas the history of ecosystems in the Western Cordillera (where the Páramo de Frontino is located) is poorly known. Nevertheless, information about the ecology and biotic diversity of montane forests and tropical alpine grasslands (called "páramos"), including those of the Western Cordillera, can be found in Cuatrecasas (1958), Rangel (1995), Gentry (1995), Rangel et al. (1997), Van der Hammen et al. (2005) and Rangel (2010), among others.

High-resolution pollen records over the last 15,000 years, which can provide reliable proxies for climate variations, are rare in the South American tropics (Flantua et al., 2015, 2016a,b; Urrego et al., 2016). Outside of Colombia, pollen records reflecting the Holocene have been well studied in Venezuela (Bradbury et al., 1981; Rull et al., 2005), Ecuador (Niemann et al., 2009; Brunschön and Behling, 2010), Peru (Weng et al., 2006) or Yucatan (Leyden, 2002). Although Colombia probably presents the largest number of palynological publications of all tropical countries (Flantua et al., 2015), very high-resolution studies (i.e., those with a time

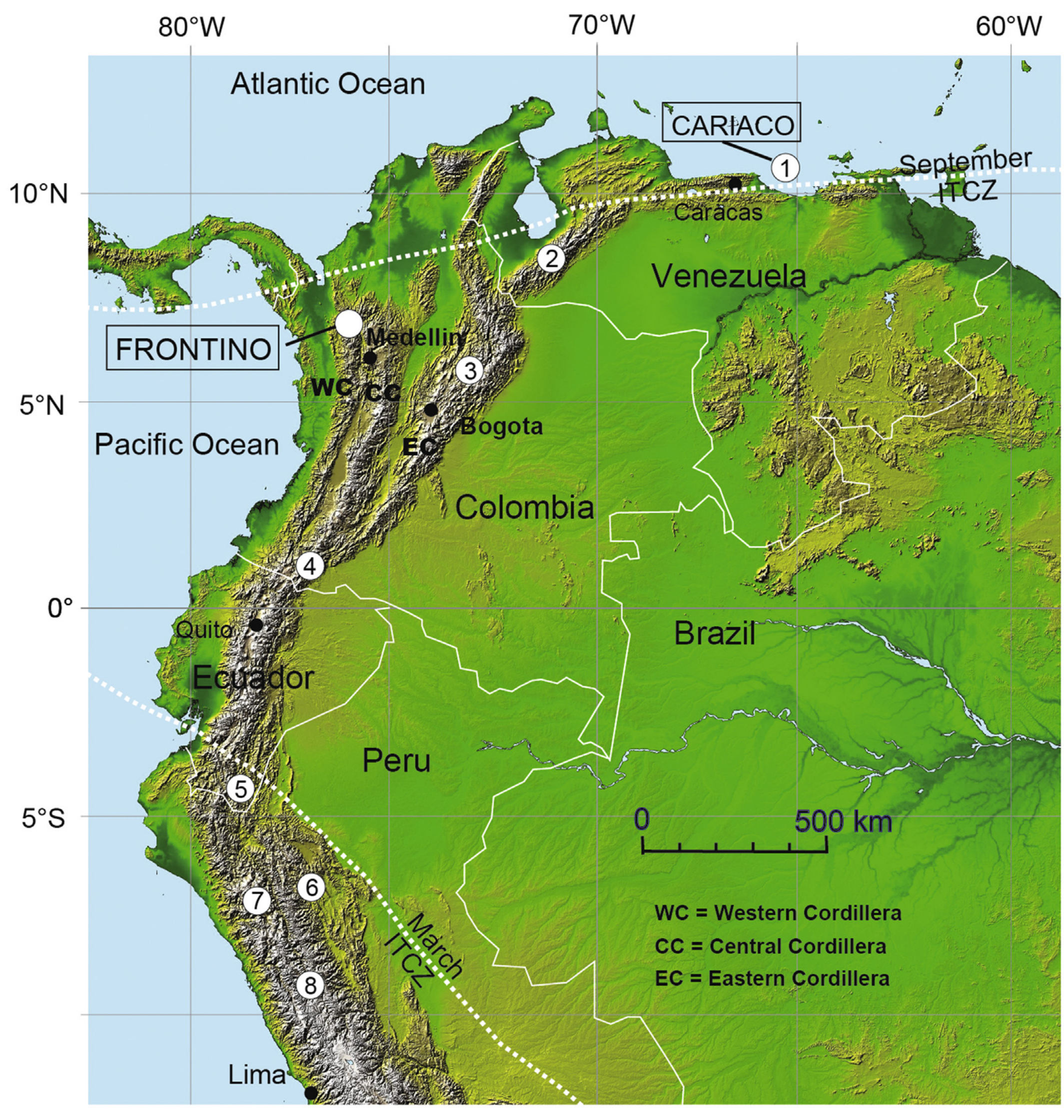

Fig. 1. Location map of the Páramo de Frontino at the northwestern termination of the Western Cordillera in Colombia and seasonal positions of the present-day Intertropical Convergence Zone (ITCZ). Locations numbered 1 to 8 show sites mentioned in the text: 1) marine Cariaco Basin, Venezuela (Haug et al., 2001); 2) Laguna Los Anteojos, Venezuela (Stansell et al., 2010); 3) Lake Fúquene, Colombia (Bogotá-Angel et al., 2011); 4) Laguna La Cocha, Colombia (González-Carranza et al., 2012); 5) Laguna Rabadilla de Vaca, Ecuador (Niemann et al., 2009); 6) Laguna de Chochos, Peru (Bush et al., 2005); 7) Laguna La Compuesta, Peru (Weng et al., 2006); 8) Huascaran ice core, Peru (Thompson et al., 1995).

resolution of less than 50 yr) are noticeably rare (Flantua et al., 2016a,b; Urrego et al., 2016): in Colombian lowlands, Wille et al. (2003) studied the last 11,000 years at Lake Las Margaritas (altitude of 290 m asl) with a time resolution of 50 yr. At high altitude, González-Carranza et al. (2012) studied the Lake La Cocha record (altitude of 2780 m asl) spanning the last 14,000 years on the Amazonian flank of the Andes in southern Colombia with a ca. 25 yr resolution. Velásquez (2005) analyzed the last 4000 years in the Llano Grande (LLG) mire in the Páramo de Frontino (altitude of 3460 m asl) with a time resolution of 20 yr, making it the first palynological study of the late Holocene in Colombia at a near-decadal timescale. Muñoz (2013) further studied palynologically the same site at near-decadal time scale down to ca. 11,500 cal yr BP. Our study uses the synthetic palynological results of the latter two authors as a palaeoclimatic proxy. Other high-altitude sites have been studied by palynology in the subtropical Andes, spanning the Lateglacial and Holocene, e.g., in Ecuador (Hansen et al., 2003), Venezuela (Rull et al., 2005) or Peru (Weng et al., 2006), but their resolution is over 100 yr. Another aspect in continental records is the stratigraphic continuity: these intervals are often affected by significant hiatuses (Van 't Veer et al., 2000; Groot et al., 2013). A continuous stratigraphical sequence with reliable age dating (Flantua et al., 2016b) is a must for high resolution. Finally, palynological data must be supported by other proxies (Flantua et al., 2015), such as geochemistry, sedimentology or other organisms (diatoms, chironomids, etc.), e.g., Vélez et al. (2001).

The high altitude and isolation of the Páramo de Frontino has preserved it from anthropogenic influences. For this reason, its geomorphology, biophysical aspects and mire sediments have been studied for the past twenty years (Jaramillo and Parra, 1993; Lozano et al., 1999; Parra and Jaramillo, 1999; Parra et al., 2010a,b,c; Velásquez et al., 1999; Velásquez, 2005; among others). The first core in the LLG mire studied in this paper was taken in 1995 and showed that the sampled sediments presented a 17 kyr long record (Velásquez and Hooghiemstra, 2013).

In this paper we present results of a multiproxy research on palaeoclimatic variability carried out on the continuous sedimentary sequence cored at the centre of the high-mountain LLG mire in the Páramo de Frontino and spanning the last 11,500 years. This study combines data from pollen (biotic proxy) and X-ray microfluorescence (μXRF, abiotic proxy). The objectives are twofold: 1) to reconstruct at a near-decadal timescale changes in the vegetation associations and inferred climate change (temperature and humidity) and compare the humidity record derived from local aquatic vegetation with the higher-resolution (sub-annual) μXRF rainfall proxy; 2) to attempt to infer the mechanisms that have driven the observed climatic variations at local and interregional scales, We compare our new data with selected high-altitude north Andean sites and a Caribbean marine site, with particular emphasis on potential connections between tropical Pacific and Atlantic climates.

2. Environmental and geological setting

2.1. Geomorphological and geological setting

The Páramo de Frontino is located at 6°29′N and 76°06′W (Fig. 1). It lies in the Department of Antioquia, some 100 km to the northwest of the city of Medellin and approximately halfway between the Pacific and Atlantic oceans. It forms the largest tropical montane grassland area in the Western Cordillera and contains several wetlands. The Páramo de Frontino corresponds geomorphologically to a large cone truncated at an altitude of ca. 3600 m asl. This high plateau is crossed by a W-E trending ridge culminating at 4080 m asl. The steep environmental gradients and short spatial distances over which communities change make this zone particularly sensitive to climate change.

Geologically, the Páramo de Frontino consists of a Tertiary dioritic to monzonitic pluton, which penetrates Cretaceous turbidites and contains volcanic rocks (basalts, andesites and tufs) also of Tertiary age (Parra et al., 2010a). The páramo flanks present steep slopes cut by deep canyons. The flat zone at the top exhibits various glacial landforms including depressions that drain eastwards (Fig. 2A). The latter were infilled by sediments during Lateglacial and Holocene times. They appear today as mires/peat bogs flooded during the wet season. The largest one studied here is the LLG mire, which lies at 3460 m asl (Fig. 2B). The area of LLG is of some 0.2 km^2 and stratigraphically continuous sediments are over 12 m thick in the central part of the basin (Fig. 2C). This study is based on cores LLG-2 and LLG-5 recovered at the depocentre. The study of Velásquez and Hooghiemstra (2013) is based on core LLG-1 taken on the flank of this basin (Fig. 2C), where the total sedimentary sequence is reduced and presents stratigraphical hiatuses.

2.2. Present-day climate

Modern climatic conditions in the Páramo de Frontino are still being poorly studied. There are no weather stations in the páramo and data come either from spot observations or from weather stations located at lower altitude and several kilometers distance (Monsalve, 2015). The climate has a typical high-altitude tropical character. It has an important diurnal range, whereas the mean monthly and mean annual temperatures (MAT) vary little. Espinal (1992) quotes MAT between 6 and 12 °C, whereas Rangel and Aguilar (1995) mention a maximum temperature of 10.5 °C, a minimum temperature of −1.9 °C and a MAT of 4.6 °C. The best estimate of MAT in LLG can be derived from stabilized soil temperatures in the Páramo de Frontino measured between 3100 and 3600 m asl (Velásquez, 2005). A value of 8.6 °C at 3460 m asl will be used as present-day MAT for the LLG location studied.

Precipitation change in Colombia is driven by the position of the ITCZ (see Fig. 1) combined with the moisture brought by the low-level Choco jet (Poveda and Mesa, 2000) in the Pacific. At annual scale, according to the data of the weather stations close to the Páramo de Frontino (Monsalve, 2015), the months of January and February are the driest of the year (southern position of the ITCZ). The second dry period lasts from June to July, with August to September slightly rainier (northern position of the ITCZ). Highest rainfall occurs usually in April, May and October, coinciding with the northward/southward progression of the ITCZ over the study area. Because the Western Cordillera partially acts as a rain shadow, its western flank receives more precipitation than its eastern flank. This annual distribution of precipitation is further affected by ENSO, marked by the Niño and Niña phenomena with a time scale of two to seven years. ENSO is the main forcing mechanism of Colombia's hydro-climatology at interannual timescales (Waylen and Poveda, 2002; Vuille and Garreaud, 2012; Flantua et al., 2016a). Overall, during El Niño events, Colombia experiences a lack of rain, and increased air temperature leads to higher evaporation. The reverse is generally valid during La Niña phases. The impact of ENSO occurs earlier and is stronger in western and central Colombia than in the east (Poveda et al., 2001).

From the data of weather stations, mean annual precipitation between 2000 and 3000 mm/year can be assumed for the study area. Finally, the high altitude, and low atmospheric pressure (less water vapour) as a consequence, make the atmosphere in the study area permeable to solar radiation.

2.3. Modern vegetation

The general altitudinal distribution of vegetation in the northern

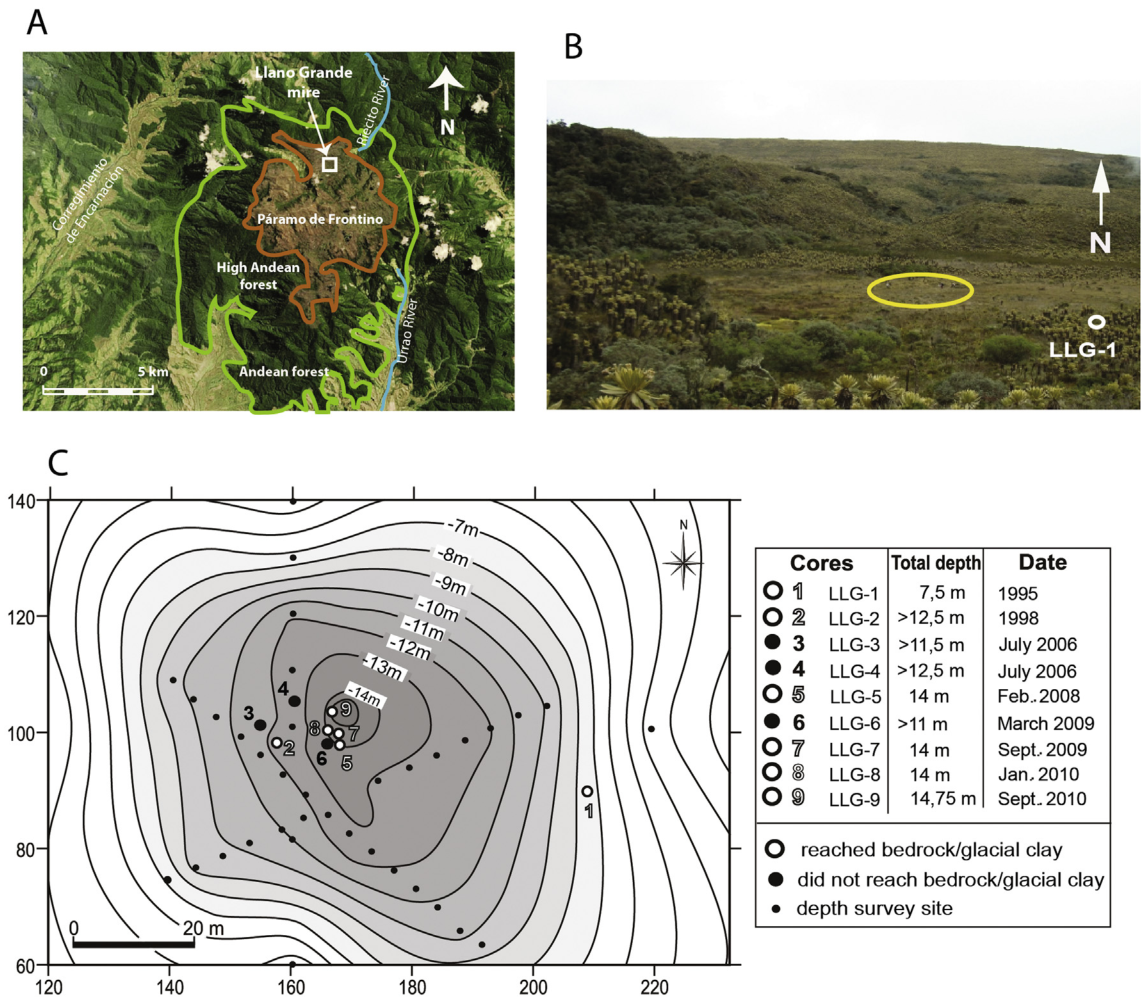

Fig. 2. The Llano Grande (LLG) mire in the Páramo de Frontino. A) Location of mire: the páramo vegetation is brown-coloured, the Andean and high-Andean arboreal forest lies between the green and brown lines (document from Bing Maps-satellite, Terraserver, 2011). B) The ca. 20 m in diameter yellow circle shows the central part of the basin where cores LLG-2 to −9 are located (photograph C. Monsalve); core LLG-1 (studied by Velásquez and Hooghiemstra, 2013) lies outside of the main depocentre. C) Depth map of the LLG Basin and location, depth and date of recovered cores. (For interpretation of the references to colour in this figure legend, the reader is referred to the web version of this article.)

Andes has been studied by Van der Hammen and González (1960a;b and 1963), Van der Hammen (1974), Cleef (1981), Rangel et al. (1982), among others. The altitudinal range of the main vegetation associations may slightly differ between the dry and wet sides of the mountains, between the Eastern and Western cordilleras, and between northern, central (Cleef and Hooghiemstra, 1984) and southern Colombia (Wille et al., 2001). The páramo vegetation in the Western Cordillera has been investigated by Rangel et al. (1999) and Cleef et al. (2005). In the Páramo de Frontino, this type of vegetation has been studied by Espinal et al. (1983), Sánchez (1998) and Rangel et al. (1999).

Many taxa show similar altitudinal ranges and justify the recognition of general vegetation zones (or vegetation belts), characterized by suites of co-occurring taxa (Table 1) forming identifiable plant associations (Bogotá-Angel, 2011). The vertical distribution of main plant associations in the Páramo de Frontino (Fig. 3A) follows that of Velásquez (2005) and Velásquez and Hooghiemstra (2013).

Ecotones are determined by environmental factors more or less well identified (Hooghiemstra et al., 2012). The transition from sub-Andean forest (or lower montane forest, Groot et al., 2011) to Andean forest (or upper montane forest, Groot et al., 2011) is mainly governed by the occurrence of night frost, which occurs mainly during dry periods (Wille et al., 2001). The transition from upper montane forest to subpáramo corresponds to the upper forest line (UFL, Fig. 3A), i.e., to the uppermost contour of closed forest (Bakker et al., 2008). Its altitudinal position is mainly governed by MAT, although changing atmospheric pCO_2 also plays a still unquantified role (Boom et al., 2002; Groot et al., 2011, 2013; Hooghiemstra et al., 2012). The factors driving the transition from shrubby subpáramo to herbaceous páramo are little known, but frost frequency and humidity probably play an important role (Hooghiemstra et al., 2012; Torres et al., 2013).

3. Material and methods

3.1. Coring and sampling

Nine cores have been taken in the LLG Basin (Fig. 2C). Following the acquisition in 1995 of core LLG-1 (Velásquez and Hooghiemstra, 2013), a depth survey of the basin was carried out. Subsequently, cores LLG-2 to LLG-9 acquired between 1999 and 2010 have been positioned closer to the centre of the basin and penetrated a much thicker section. Cores LLG-2 to LLG-9 have been recovered using a hand-operated “Russian” corer. It cuts 50-cm long half-cylindrical cores with a diameter of 5 cm. This device has the great

Table 1
Taxa recognized in the palynological study of the Páramo de Frontino. Taxa are grouped according to ecological (see Fig. 3A). Aquatic taxa are grouped according to their preference in relation to water depth (see Fig. 3B).

Regional vegetation		Local vegetation (aquatics)	
Altitudinal range	Taxa	Group (water depth range)	Taxa
SubAndean (or **lower mountane forest**) (~1000–2100 m asl)	*Acalypha, Alcornea*, Bignonaceae, *Cecropia*, Fabaceae, Mimosaceae, *Pilea, Sapium*, Urticales	**Submerged** (40–80 cm)	*Isoetes*
Andean (or **upper montane forest**) (2100–3450 m asl)	*Alnus*, Araliaceae, *Ardisia,Bocconia, Clethra, Clusia*, Cyatheaceae, *Drimys, Eugenia, Gaiadendron, Hedyosmum, Hesperomeles, Ilex, Juglans*, Melastomataceae, *Miconia, Mirica, Myrsine*, Myrtaceae, *Pinus, Podocarpus, Prunus*, Solanaceae, *Symplocos, Thalictrum, Vallea, Viburnum, Weinmannia*	**Marsh** (0–20 cm)	Apiaceae, Cyperaceae,Hydrocotyle, *Lachemilla,Ranunculus*
Subpáramo (3450–3550 m asl)	Asteraceae, Ericaceae, *Polylepis*	**Cushion** (0 cm)	*Plantago*
Páramo (3550–4100 m asl)	*Aragoa, Arcytophyllum, Blechnum* Caryophyllaceae, Gentianaceae, *Geranium, Hypericum*, Lamiaceae, Lycopodiaceae, Poaceae, *Rumex, Sisyrincum, Valeriana*		

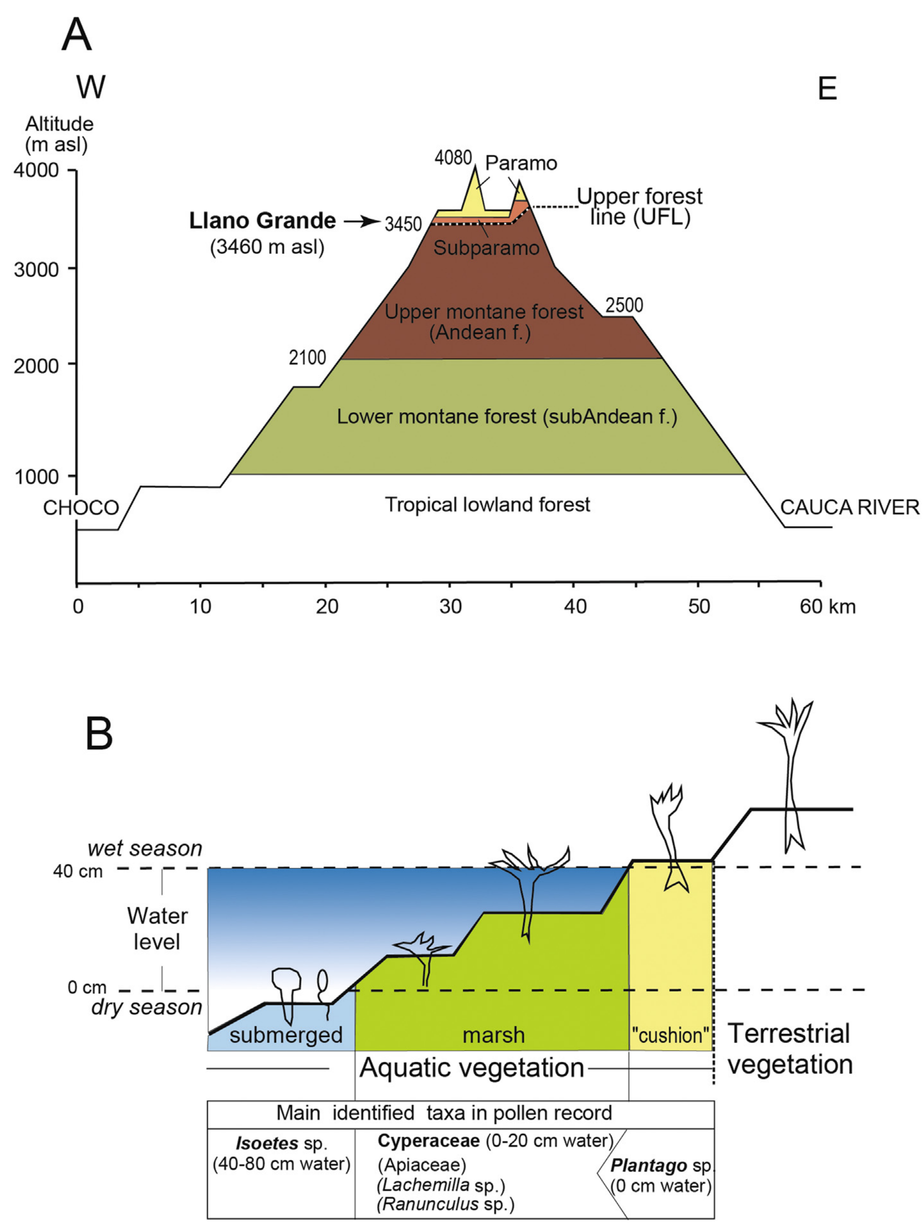

Fig. 3. A) Present-day altitudinal vegetation distribution in the Western Cordillera of Colombia showing the main vegetation zones (modified after Velásquez and Hooghiemstra, 2013). The changing position of the upper forest line (UFL) is used as a proxy for temperature change (see text). B) Present-day distribution of the aquatic vegetation used as a proxy for water level changes and inferred precipitation (after Parra et al., 2010b).

advantage of not compacting sediments, because once set in the subsurface at the desired depth it cuts off the sediments horizontally. Cores LLG-6 to LLG-9 (Fig. 2C) have been recovered twice, the twin cores being separated by less than 50 cm. The twin cores LLG-9 have been vertically displaced of 25 cm to insure a full continuity of the sediments.

Cores LLG-2, -5, -7, -8 and -9 have reached glacial clays or bedrock below a thick organic-rich sequence. All cores have been photographed in the field. Cores LLG-2 to −4 have been studied in detail in the field, particularly core LLG-2 (Parra et al., 2010c), and sampled at 1 cm increments for palynological studies. Cores LLG-5 to −9 have been packed in plastic half tubes and carried to the National University of Colombia in Medellin for further studies. Core LLG-5 has been further sampled using U-channels and subsequently studied at the University of Geneva (Switzerland) both for μXRF and lithology.

The present research is based on cores LLG-2 for palynology and LLG-5 for geochemistry. Samples used for ^{14}C analyses come from cores LLG-2, -3, -4, -5 and -8 in the central part of the basin.

3.2. Palynology

3.2.1. Processing, counting and result display

Palynological data used in this study (Velásquez, 2005; Muñoz, 2013) all come from core LLG-2 (Fig. 2C). All samples have been prepared at the Palaeoecology Laboratory of the National University of Colombia (Medellin). Velásquez (2005) has studied the upper 220 cm of the core with samples taken at 1 cm increments. Muñoz (2013) has studied the same core from 220 cm down to 754 cm with samples taken at 2–3 cm increments.

Sediment samples of 1 cm^3 have been treated with standard pollen preparation procedures including potassium hydroxide and acetolysis (Faegri and Iversen, 1989). One tablet of exotic *Lycopodium* spores has been added to each sample for calculation of the pollen concentration values. Pollen samples have been mounted in glycerin gelatin, and slides sealed with wax. Pollen grains from the regional vegetation have been included in the pollen sum and ecologically grouped according to the different vegetation zones (Table 1, Fig. 3A). Pollen from aquatics and undetermined pollen grains, algal colonies and fern and fungal spores have been excluded from the pollen sum. In the Páramo de Frontino, local vegetation consists essentially of aquatic plants, for which an environmental model has been established by Parra et al. (2010b) (Table 1, Fig. 3B). For the pollen sum, a minimum of 300 pollen grains has been counted by Velásquez (2005) for the interval of 0–220 cm in core LLG-2, whereas Muñoz (2013) has counted all pollen and spores in 21 μml of pollen solution for the interval 220–754 in the same core. In both studies, pollen and spore assemblages are comparable and the relative proportions of taxa can be compared and merged into one single composite pollen record covering the interval 0–754 cm. For pollen and spore identification, Velásquez (2005) and Muñoz (2013) have used Hooghiemstra (1984), Kuhry (1988), Roubik and Moreno (1991), Salomons (1986) and Velásquez (1999), as well as the reference collections at the Palaeoecology Laboratory of the National University of Colombia in Medellín and at the Institute for Biodiversity and Ecosystem Dynamics (IBED) of the University of Amsterdam (Netherlands).

Percentage calculations and data plotting have been carried out using the software TILIA and TILIAGRAPH (version 2.0.2, Grimm, 1987).

3.2.2. Use of pollen data as palaeoenvironmental and climatic proxy

Van der Hammen and González (1960a,b and 1963) defined the UFL as the uppermost and mainly continuous boundary between the about 5 m high or taller forest vegetation and the dwarf forest belt (subpáramo). Isolated forest patches, small dwarf forest at higher altitudes in wind-protected valleys should not be taken into account. The concept of shifting UFL has been widely applied to reconstruct palaeotemperatures (e.g., Hooghiemstra, 1984, 1989; Hooghiemstra and Ran, 1994; Mommersteeg, 1998; Van 't Veer and Hooghiemstra, 2000; Wille et al., 2001; Torres, 2005; Bogotá-Angel, 2011; Groot et al., 2011; Hooghiemstra et al., 2012).

The percentage of arboreal pollen (AP%) reflects the altitudinal position of the UFL, each 5% change in AP% corresponding to a 100 m shift of the UFL (Hooghiemstra, 1984; Van 't Veer and Hooghiemstra, 2000; Bakker et al., 2008; Groot et al., 2011; Velásquez and Hooghiemstra, 2013; Groot et al., 2013). As mentioned before, the position of the UFL is largely determined by the MAT (Groot et al., 2011, 2013). Because there are no studies in the Western Cordillera about lapse rates, a lapse rate of 0.6°C/100 m forest displacement has been chosen for the study site (Velásquez and Hooghiemstra, 2013). The present-day UFL in the Páramo de Frontino can be estimated at 3450 m asl (Rangel et al., 1999; Velásquez, 2005). The palynological data of Velásquez (2005) in LLG show that the present-day AP% is ca. 53% at 3460 m asl at the study site. We have used the present-day stabilized soil temperature of 8.6 °C (Velásquez, 2005) as the best estimate of MAT at the elevation of the mire (3460 m asl). Using these parameters and the AP%, we have estimated the elevation of the UFL and the MAT with the following relations (1) and (2):

$$UFL = 3450 + \left[\frac{(AP\% - 53)}{5}\right] \times 100 \quad (1)$$

$$MAT = 8.6 + \left[\frac{(UFL - 3450)}{100}\right] \times 0.6 \quad (2)$$

Where:

UFL = upper forest line in meters; 3450 = present-day altitude (m asl) of UFL; value of 53 = present-day AP% at 3460 m asl (elevation of study area); values of 5 and 100 = each 5% change in AP% corresponds to an UFL shift of 100 m; MAT = mean annual temperature (°C) at mire elevation; 8.6 = present-day MAT (°C) in the study area; value of 0.6 = lapse rate of 0.6°C/100 m forest displacement.

Velásquez and Hooghiemstra (2013) have used slightly different values of present-day MAT (9.5 °C) and AP% (40%), but these differences do not affect significantly the relative changes in UFL and MAT over time.

Varying proportions of local aquatic vegetation are indicative of changing water levels in the mire and can be used as a proxy for rainfall (e.g., Hooghiemstra, 1984, 1989; Van 't Veer and Hooghiemstra, 2000; Torres et al., 2005; Bogotá-Angel, 2011; Van Boxel et al., 2014; Urrego et al., 2016). In LLG the local aquatic vegetation includes deep water plants, marsh and cushion vegetation (Table 1). The ecology of the modern aquatic and marsh vegetation in the Páramo de Frontino has been studied by Parra et al. (2010b). This model can be applied to estimate the water depth of the LLG lake (Fig. 3B), using relation (3):

$$\text{Water Depth} = \frac{(\%\mathit{Isoetes} \times 60) + (\%\mathit{Cyperaceae} \times 10) + (\%\mathit{Plantago} \times 0.1)}{100} \quad (3)$$

Where:

Water depth = estimated water depth of the mire (cm); values of 60, 10 and 0.1 = average water depth in cm corresponding to respective taxa according to the model of Fig. 3B (in the marsh vegetation, only the Cyperaceae have been used because they are dominant).

3.3. X-ray fluorescence (XRF)

Recognizing chemical elements in lake sediments may provide significant climate and environmental information. In this respect, Jansen et al. (1998) have developed a non-destructive logging technique applying XRF for the determination of major-element concentrations in split sediment cores. Because of the high resolution of its semi-quantitative records, XRF is a useful tool for detailed time-series analysis (e.g., Jansen et al., 1998; Röhl and Abrams, 2000; Helmke et al., 2005). The principal advantage of this technique is the acquisition of high-resolution semi-continuous measurements, which can be carried out rapidly in a non-destructive way.

Elemental analysis has been performed on the LLG-5 core using the EDAX Eagle III XPL μProbe at the Earth Science Department of the University of Geneva. Because of the extremely high resolution of this instrument (μProbe), the high-density data acquired will be referred to as X-ray microfluorescence (μXRF) data. This allows the distinction from standard XRF data acquired with lower resolution devices. Material for μXRF analyses has been sampled at the National University of Colombia in Medellín in 50 cm-long U-channels from the cores recovered with the Russian corer (see above) and transported to the University of Geneva. The U-channels have been cut into 10 cm long sections to be analyzed in the Eagle III spectrometre. Some 180 to 200 points have been measured for each 10 cm segment of the LLG-5 core down to a depth of 14 m. Only the results that are time-equivalent to the interval covered by the palynological data in core LLG-2 (i.e., 0–754 cm) are presented here. Parameters used for measurements have been set at 40 kV, 450 μA, 50/55 Dtm at atmospheric pressure. Two profiles over the same sections have been acquired in various parts of the core, giving consistent results. Measured values are expressed in counts per second (cps). According to the manufacturer, the lowest level of reliability is at around 7cps.

The elements present in the mineral fraction of sediments come essentially from running waters in the catchment area of the LLG lake, where the bedrock is made principally of volcanic rocks (andesites, basalts and volcanic tufs). An ultra-high resolution record for Fe and Ti has been obtained. Ti is a very conservative element and should be preferred as a proxy for rainfall in the catchment area (e.g., Haug et al., 2001; Petersen and Haug, 2006). Although less conservative, Fe can also be used if not affected by diagenesis (Petersen et al., 2000). This is the case in our study, where the Fe curve is fairly similar to that of Ti and will be used in the upper part of the late Holocene where Ti measurements are less reliable because of their low values.

3.4. Statistics

The main aim of wavelet analysis (e.g., Weng and Lau, 1994; Torrence and Compo, 1998) is to determine the frequency content of a signal and to assess the temporal variation of the frequency content. The wavelet transform allows for tracking the time evolution of processes at different scales in the signal. It has been used extensively in geosciences, e.g., to analyze meteorological data, ocean and land temperatures, precipitation data, influence of ENSO on tropical river discharge, etc … (Labat, 2005). In this study, wavelet analysis has been carried out on Ti and Fe data to obtain time series and try to identify significant periods (amount of time for a cyclic phenomenon to repeat itself) during the Holocene. It has been used to evaluate the time series of red colour intensity for statistically significant variance. This method has been chosen because of its use on non-stationary signals. By employing the adequate wavelet, it can provide excellent time and frequency localization. Wavelet spectra have been calculated over the last 12,000 cal yr BP (ca. 19,000 measurements) of the red colour intensity time series using a continuous wavelet transform with significance testing. The chosen continuous Morlet wavelet (Farge, 1992; Yi and Shu, 2012) has been used to calculate the wavelet power spectra and to identify changes in variance within selected frequency time bands trough time.

The desktop operating system used is UBUNTU 11.10, which is based on the Debian Linux distribution and is shared as free and open source software, using its own desktop environment. The statistical software used is the open source R language (version 2.14; Fox and Andersen, 2005). Finally, the program PAST has been used to generate the Morlet wavelet and wavelet power spectrum. This program is designed as a follow-up to PALSTAT, an extensive package written by Ryan et al. (1995). It includes a number of functions commonly used in palaeontology and palaeoecology.

4. Results

4.1. Lithology

Lithological studies have been carried out on core LLG-2 by Parra et al. (2010c) and on core LLG-5 in relation with the μXRF study. The other cores have been studied to establish a precise lithological correlation (Fig. 4). Although this study covers only the upper part of cores LLG-2 and -5 (down to just below the limit between lithological units 2 and 3, Fig. 4), it is important to present here the lithology of the whole stratigraphical section, which has been used to establish the age model of the Lateglacial and Holocene infill.

Three lithological units are distinguished in the LLG basin. The lowermost Unit 1 (Fig. 4) consists of light grey-white mineral mud with some dark laminae in the upper part. In core LLG-5, the basal part contains coarse grains of plagioclases indicating the proximity of the basin bedrock. The limit between units 1 and 2 is marked by an unconformity.

Unit 2 is made of dark brown organo-mineral mud. Its lower part is rich in diatoms (Fig. 4) and contains at its base several tephra levels. The upper part of Unit 2 has a similar lithology, but is poor in diatoms (Fig. 4). The top of the organo-mineral Unit 2 is another important marker for the correlation of cores. It marks a sudden transition to sediments made essentially of vegetal filaments and fragments with little mineral content apart from diatoms. This change occurs at 8.5 m in LLG-5 and 7.43 m in LLG-2. Although this transition is rapid, there is no indication in any of the cores of an unconformity at this level. The stratification remains horizontal and there are no indications of a major hiatus. The difference in depth between LLG-2 and LLG-5 reflects a microtopography in the basin and/or could be explained by differential compaction of underlying sediments. The two cores are ca. 11 m apart.

Unit 3 is made of dark brown peat and organic mud very rich in vegetal filaments and fragments. Its lower part is extremely rich in diatoms (Fig. 4), which can locally make up to 90% of the sediments. These diatomites have a lighter brown colour. The upper part of Unit 3, i.e., the uppermost 6 m or so of all cores (except LLG-1) present an identical lithology made of diatom-poor peat and organic mud (Fig. 4). Within this interval, the only marker is a few centimetres thick intercalation of volcanic ashes situated at a depth of around 4 m.

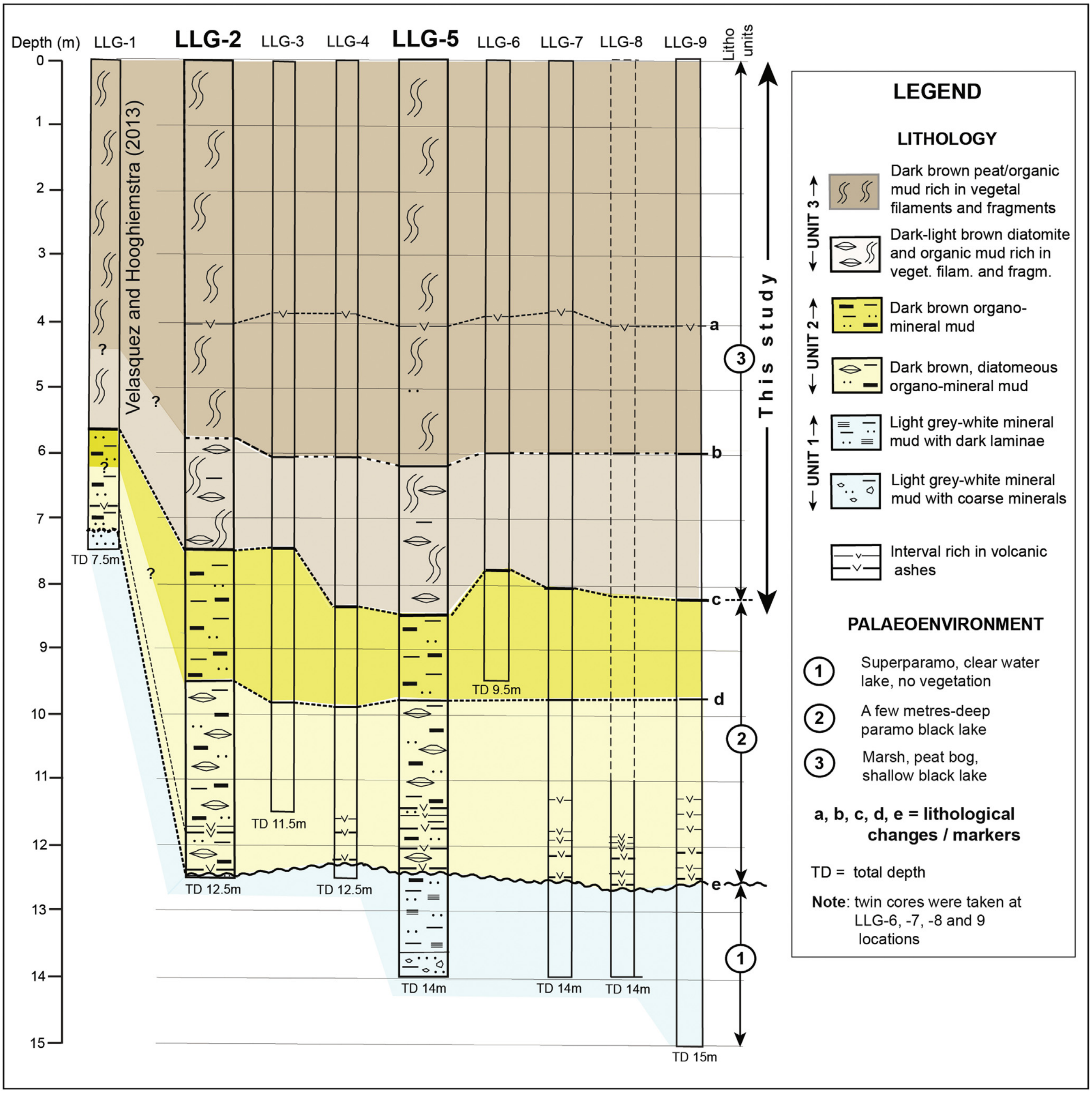

Fig. 4. Lithology and depositional environment of sediments in the LLG basin based on cores LLG-1 to −9: in this study palynological data come from core LLG-2 and X-ray microfluorescence (μXRF) data from core LLG-5. This paper covers essentially palaeoenvironmental zone 3. Correlation lines labelled "*a, b, c, d* and *e*" correspond to major lithological changes/markers; in the central part of the basin, where cores LLG-2 to −9 are located, they are considered as isochrons (used to calibrate the age model for LLG-2 data, see Suppl. Fig. 1).

Lines *a* to *e* in Fig. 4 correlate the main lithological changes observed in the sedimentary sequence. In the central part of the basin, where the sequence is complete and cores LLG-2 to LLG-9 close to each other, these lines correspond to isochrons. Correlation with core LLG-1 studied by Velásquez and Hooghiemstra (2013) must be considered with caution. This first core was acquired on the flank of the basin (Fig. 3B) and its total thickness is about half of that encountered at the centre of the depression. It corresponds to a condensed section and is likely to present hiatuses. Moreover, it has been cored with a Dachnovsky sampler that compacts sediments. Consequently, it is difficult to correlate with the type section consisting of LLG-2 and 5.

4.2. Age model

The age model (Fig. 5) is based on 30 Accelerator Mass Spectrometry (AMS) ^{14}C measurements carried out on samples recovered in the central part of the basin (Table 2). Those carried out at the Poznan Laboratory in Poland (13 samples) have been calibrated using the program CALIB 5.0 (two-sigma calibration values). This program was updated from CALIB 3.0 (Stuiver and Reimer, 1993) and CALIB 4.0 to use the INTCAL04 data set (Reimer et al., 2004).

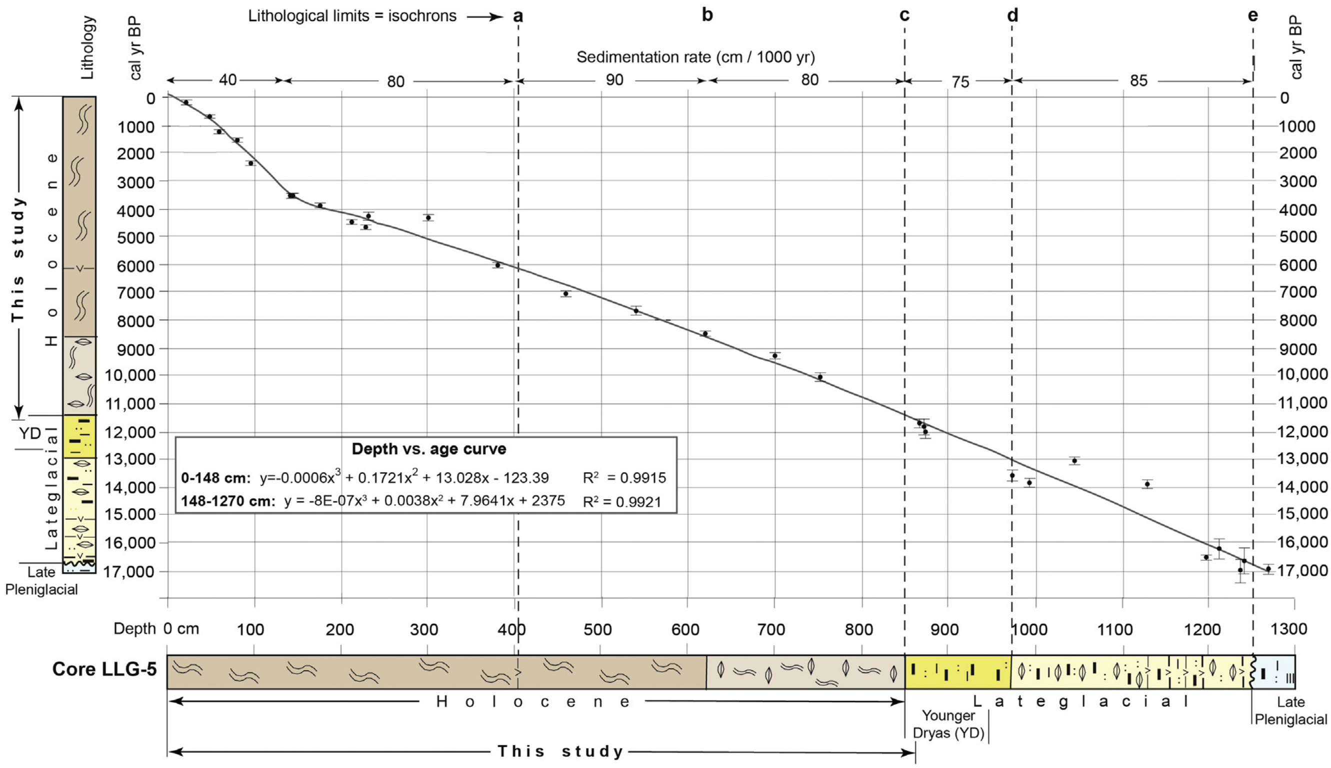

Fig. 5. Age model for the LLG Basin. This model is based on 30 AMS ^{14}C datings (see Table 2) and is representative for the central part of the basin (Fig. 2C) where core LLG-5 is located (see text for explanation). This model has been used to convert µXRF sample depth from core LLG-5 to age. See Fig. 4 for lithological legend. Lines labelled *a*, *b*, *c*, *d* and *e* correspond to isochrons in the central part of the basin (Fig. 4). From surface down to time line *a* (at a depth of about 4 m), this model can also be applied directly to the palynological data in core LLG-2. Isochrons *b*, *c* and *d* are not at the same depth in cores LLG-5 and LLG-2 and the model has been slightly adapted to convert palynological sample depth from core LLG-2 to age (see text and Suppl. Fig. 1 for explanation).

Table 2
Radiocarbon ages and bulk sample specific information (see Fig. 5 and Suppl. Fig. 1).

Core	Interval (cm)	Av. depth (cm)	^{14}C age (cm)	Deviation (±)	Cal yr BP (Intcal04)2σ	Deviation (±)	δ^{13}C (o/ooPDB)	C^{14} Lab	Dated material
LLG-2	19–21	20	130	30	170	110	–25	Poz-235	Peat
LLG-5	50–53	51.5	770	40	700	40	–27.6	Beta-259,645	Fibrous organic mud
LLG-2	58–61	59.5	1280	30	1230	60	–25	Poz-236	Fibrous organic mud
LLG-2	76–80	78	1600	30	1480	70	–25	Poz-237	Peat
LLG-2	94–98	96	2370	35	2410	75	–25	Poz-238	Fibrous organic mud
LLG-2	139–148	143.5	3340	35	3560	85	–25	Poz-251	Fibrous organic mud
LLG-5	140–142	141	3330	40	3570	110	–24.3	Beta-259,646	Fibrous organic mud
LLG-2	175–178	176.5	3630	35	3930	80	–25	Poz-232	Peat
LLG-2	211–214	212.5	4030	35	4490	70	–25	Poz-250	Fibrous organic mud
LLG-2	228–230	229	4120	40	4670	150	–25	Poz-239	Fibrous organic mud
LLG-5	230–233	231.5	3890	40	4290	130	–25.7	Beta-259,647	Fibrous organic mud
LLG-5	300–303	301.5	3910	40	4335	95	–26.2	Beta-259,648	Fibrous organic mud
LLG-5	380–383	381.5	5230	40	6045	125	–24.7	Beta-259,649	Fibrous organic mud
LLG-5	460–463	461.5	6170	50	7090	150	–25.6	Bata-259,650	Fibrous organic mud
LLG-5	540–543	541.5	6830	50	7665	85	–25.3	Beta-259,651	Fibrous organic mud
LLG-5	620–623	621.5	7730	50	8505	95	–26.3	Beta-259,652	Fibrous organic diatom. mud
LLG-5	700–703	701.5	8280	50	9280	160	–25	Beta-259,653	Fibrous organic diatom. mud
LLG-5	752–754	753	8910	50	10,045	155	–26.1	Beta-259,336	Fibrous organic diatom. mud
LLG-5	866–868	867	10,080	50	11,685	295	–24.8	Beta-246,337	Organo-mineral mud
LLG-5	872–874	873	10,150	50	11,830	220	–25.6	Beta-246,338	Organo-mineral mud
LLG-3	874–876	875	10,280	60	12,030	215	–29.1	Poz-21086	Organo-mineral mud
LLG-3	974–976	975	11,740	70	13,590	170		Poz-21087	Organo-mineral mud
LLG-3	994–996	995	11,980	70	13,860	150		Poz-21088	Organo-mineral diatom. mud
LLG-5	1046–1048	1047	11,120	60	13,040	140	–27	Beta-246,339	Organo-mineral diatom. mud
LLG-8	1130–1134	1132	11,950	100	13,905	105	–26.6	Beta-286,835	Organo-mineral mud
LLG-5	1197–1200	1198.5	13,850	70	16,505	365	–27	Beta-259,656	Organo-mineral mud
LLG-4	1212–1214	1213	13,590	90	16,190	430		Poz-21090	Organo-mineral mud
LLG-4	1237–1239	1238	14,210	90	16,970	460		Poz-21091	Organo-mineral mud
LLG-8	1240–1243	1241.5	13,940	70	16,610	180	–28.9	Beta-278,833	Organo-mineral mud
LLG-8	1266–1274	1270	14,170	70	16,910	175	–27.8	Beta-278,834	Organo-mineral mud

The other 17 AMS datings have been performed at the Beta-Analytic Laboratory in Florida, which provides both conventional radiocarbon and two-sigma calibrated ages. The latter calibration uses the INTCAL04 database and the mathematics of Talma and Vogel (1993). Datings in core LLG-2 have been obtained in an earlier research (Parra, 2005; Velásquez, 2005), and those in cores LLG3, -4, -5 and -8 in the framework of the present study.

Two third grade polynomial functions have been used to accommodate the very low sedimentation rate of the upper 150 cm of the cores. In this upper part, datings from LLG-2 complemented by those of LLG-5 give a very accurate function (Fig. 5). Another function has been obtained using data from 150 to 1270 cm. These two functions merge perfectly at 148 cm and form the continuous depth vs. age curve shown in Fig. 5. This curve gives an accurate age model to convert from depth to age both μXRF data in core LLG-5 and palynological data in core LLG-2 down to isochron *a* at 405 cm (Fig. 4). Below isochron *a* down to a depth of about 9 m, the age vs. depth curve is based only on datings from LLG-5 (Fig. 4, Table 2). Below 9 m down to isochron *e* (Fig. 4), the curve is also based on datings from LLG-3, -4, and -8 (Table 2), but the correlation shows that there are little thickness variations between these cores and LLG-5 in this interval. Therefore, between isochrons *a* and *e* (Figs. 4 and 5), the age model is directly applicable to convert μXRF levels from depth to age in core LLG-5. As for the depth to age conversion of palynological data in core LLG-2 between isochrons *a* and *e*, some adjustments to the LLG-5 age curve are needed, particularly at the level of isochron *c* where there is about 1 m depth difference between cores LLG-5 and LLG-2 (Fig. 4). This adjustment is made using linear functions between isochrons *a* and *e*, thereby providing a depth vs. age curve that can be specifically applied to the LLG-2 palynological data below 405 cm (Suppl. Fig. 1).

The age model (Fig. 5) shows that the sedimentary section from isochron *e* to the surface represents a continuous record spanning the last 17,000 years, i.e., the Lateglacial and Holocene periods. In this study, the top of the Younger Dryas equivalent (YD)/base Holocene has been chosen at the level of isochron *c* (dated at about 11,410 cal yr BP) for the following reasons (Van 't Veer et al., 2000): (1) isochron *c* corresponds to a major lithological change from an organo-mineral mud (characterizing the Lateglacial deglaciation phase) to an organic sediment rich in vegetal filaments and fragments; (2) it corresponds to a major climatic change (see sections 4.3 and 4.4) both in temperature and humidity; (3) this limit falls within the YD chronozone.

The present study covers the topmost part of the Lateglacial, i.e., the YD from an age of about 11,490 cal yr BP, and the whole Holocene period (Fig. 5). The oldest palynological sample studied is at a depth of 754 cm in core LLG-2, which corresponds to a depth of 857 cm in core LLG-5 where μXRF analyses have been carried out (Suppl. Fig. 1).

Sedimentation rates in the Lateglacial and most of the Holocene vary between 75 and 90 cm/1000 yr (Fig. 5). Sedimentation is reduced down to 40 cm/1000 yr during the last 3500 years, corresponding essentially to peat formation.

4.3. Pollen analysis

In our study we use the high-resolution palynological studies carried out at the centre of the basin in core LLG-2 by Velásquez (2005) and Muñoz (2013). Velásquez (2005) studied one sample every centimetre between 0 and 220 cm and Muñoz (2013) one sample every 2–3 cm between 220 and 754 cm. Using the age model of core LLG-2 (Suppl. Fig. 1), the time resolution of the palynological data can be estimated at ca. 25 yr for the interval 0–3500 cal yr BP, ca. 10 yr for the interval 3500–4300 cal yr BP and ca. 35 yr for the interval 4300–11,490 cal yr BP.

Palynological results of Velásquez (2005) and Muñoz (2013) for the regional vegetation and the aquatics are presented in Fig. 6 (first and third diagram from the left). In the percentage diagram, the UFL corresponds to the transition from upper montane forest to subpáramo vegetation. Using the AP% curve, we have calculated altitudinal shifts of the UFL using relation (1) described above (Fig. 6, second diagram from the left). From the altitude of the UFL and using relation (2) we have also estimated the MAT for the past at the mire elevation. From the diagram of the aquatics and using relation (3), we have estimated the mire water depth variation for the past (Fig. 6, fourth diagram from the left). Using the percentage diagram, we have visually subdivided the record in *seven intervals*, the limits of which correspond to significant changes in the altitudinal distribution of montane forest and páramo vegetation (Fig. 6).

Interval 1 represents the uppermost part of the YD (equivalent to the Colombian El Abra stadial, Van der Hammen and Hooghiemstra, 1995; Van 't Veer et al., 2000). Palynological proxies point to a cold and wet climate with a MAT some 3.5 °C and an UFL about 600 m below the present-day levels. The transition from YD to Holocene at about 11,410 cal yr BP is marked by the sharpest increase in AP% of the whole record. The MAT may have increased by some 3.5 °C and the UFL by some 600 m up to a level similar to the present-day one at 3450 m asl. A sharp transition is also observed in the local aquatic vegetation pointing to a rapid decrease in the water depth of the mire (Fig. 6). During *interval 2*, the UFL altitudinal level remained high until about 10,700 cal yr BP, accompanied by dry conditions. During the following 1000 years until about 9700 cal yr BP (*interval 3*), the UFL went down by about 350 m which corresponds to a drop in MAT of some 2–2.5 °C. The water level in the mire remained very low. *Interval 4 (*9700–6900 cal yr BP) is marked by an overall elevation of the UFL and MAT close to present-day values. A slightly colder phase occurred between ca. 8100 and 7500 cal yr BP with a peak of dryness in the upper part leading to the desiccation of the lake. *Interval 5* (6900–4000 cal yr BP) is marked by an overall decrease in the elevation of the UFL down to about 3000 m and in the MAT down to about 2.5 °C below the present-day value. This decrease in temperature is accompanied by an increase in water depth of the mire culminating between 5000 and 4000 cal yr BP. During *interval 6* (4000–2400 cal yr BP) the UFL reached its highest altitude of the record (Fig. 6). Two warm pulses can be recognized: a short one at the base of the interval (4000–3800 cal yr BP) is accompanied by drier conditions; a longer (3500–2600 cal yr BP) and warmer one, during which the UFL may have gone up to 3900–4000 m, which indicates a MAT up to 3 °C higher than today. This second warm spell was accompanied by very dry conditions that probably led to the dessiccation of the lake. These two warm periods are separated by a cold and wet interval (3800–3500 cal yr BP), during which the water depth of the lake increased to a level similar to that in the upper part of interval 5 (Fig. 6). *Interval 7* covers the last 2400 cal yr BP. It shows a sudden drop in altitude of the UFL at around the limit with interval 6, and this trend of lowering temperatures continues until ca. 1200 cal yr BP. These apparently cold conditions were accompanied between 1800 and 900 cal yr BP by an increase in the estimated water depth of the mire (Fig. 6). From about 900 cal yr BP until today, the altitude of the UFL increased fairly regularly to reach its present-day level, together with a rapidly decreasing water depth of the mire.

4.4. Microfluorescence-X (μXRF)

Ti and Fe records have a sub-annual (ca. 6-month) time resolution, with ca. 19'000 measurements each over the first 857 cm of core LLG-5. Ti and Fe data have been smoothed through a 14-point

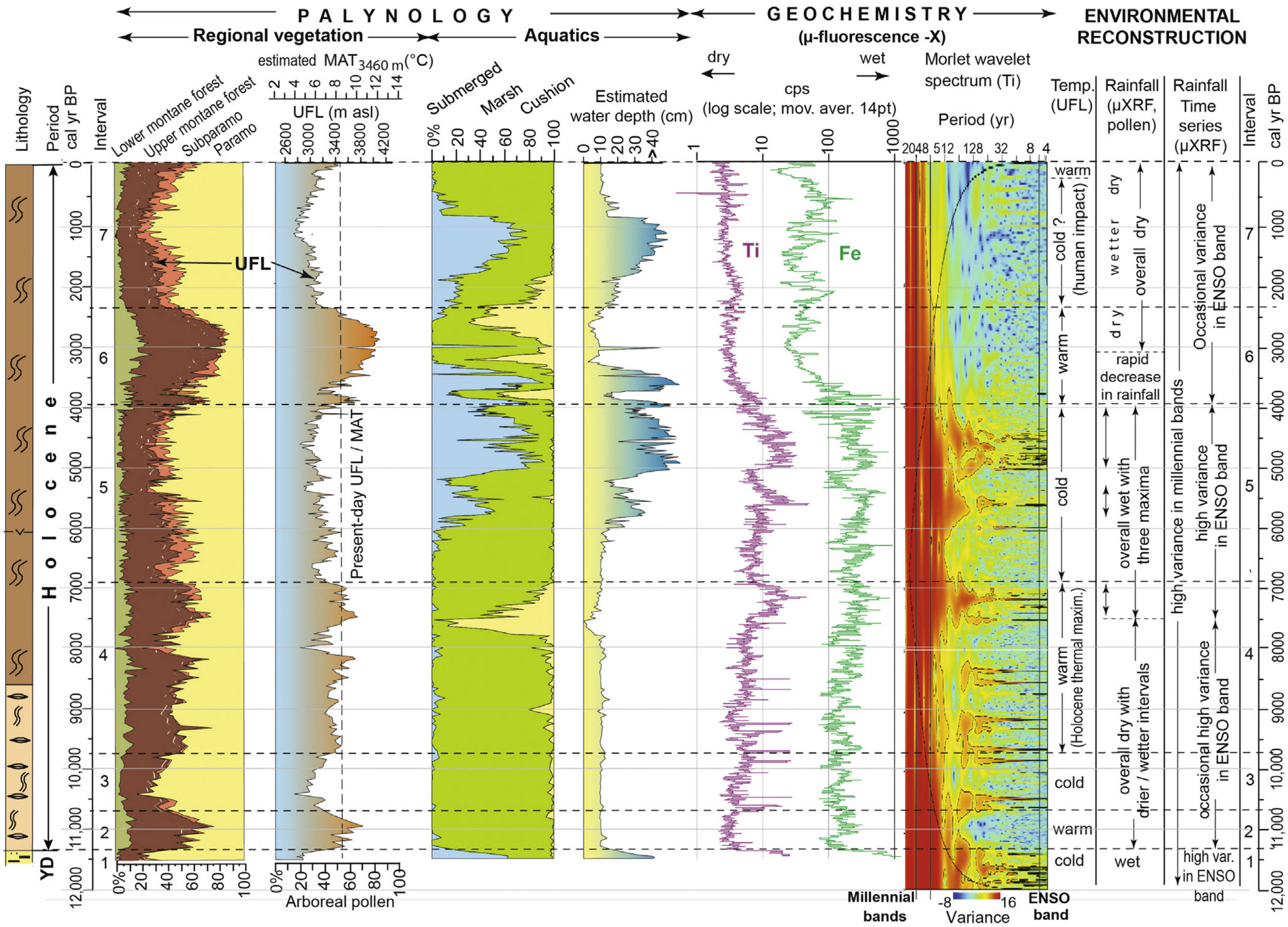

Fig. 6. Palynological (core LLG-2) and X-ray microfluorescence (µXRF, core LLG-5) results for the Holocene and late Younger Dryas (YD). Records of upper forest line (UFL) and mean annual temperature (MAT, inferred from AP% record), water depth (inferred from aquatic vegetation record) and of Ti and Fe (µXRF-based). The time series analysis using the Morlet wavelet spectrum shows frequencies for Ti (see text for explanation); it has been carried out over the last 12,000 years and uses the original µXRF data at sub-annual time scale; the moving average 14 pt has been used only for display purposes. At the right hand side a synthesis of environmental conditions.

moving average for display purposes and are plotted as indicative of wet vs. dry conditions (Fig. 6). The two curves show a high degree of similarity. We shall concentrate on the curve of the very conservative Ti, except in the upper part of the late Holocene where Ti values are below the threshold of reliability.

The upper part of the YD (*interval 1*) is characterized by high Ti values indicative of important rainfall. The transition from *interval 1 to 2* (i.e., from YD to Holocene at ca. 11,410 cal yr BP) is marked by a sudden drop in Ti values, i.e., a rapid decrease in rainfall, which remained low during *interval 2*. Low values of Ti in *interval 3* are indicative of low rainfall and these dry conditions persisted in *interval 4* with some minor variations until ca. 7500 cal yr BP. The uppermost part of *interval 4* between 7500 and 7000 cal yr BP is marked by a peak in rainfall. *Interval 5* is marked by an overall increase in the Ti signal with two maxima, one at around 5700 cal yr BP and the other one between ca. 5000 and 4200 cal yr BP, which corresponds to the highest rainfall level during the Holocene. The Ti values start decreasing towards the top of interval 5, implying decreasing rainfall. *Interval 6* (4000–2300 cal yr BP) is characterized by a rapid drop in the Ti values, indicative of a rapid decrease in rainfall. During *Interval 7* (2300- present-day) the values of Ti are too low to be interpreted, and the Fe record can be used instead. It indicates an overall low level of precipitations with some slightly wetter phases.

5. Interpretation and environmental reconstruction

5.1. Lithology

The threefold subdivision of the sedimentary sequence penetrated at the centre of the LLG Basin (Fig. 4) corresponds to major palaeoenvironmental changes. Unit 1 (tested by cores LLG-4, -5, -7,-8 and -9) is interpreted as periglacial deposits, probably corresponding to the phase of glacier melting. This type of environment is encountered in present-day superpáramo clear-water lakes like those encountered in the Sierra Nevada del Cocuy in the Eastern Cordillera of Colombia (N. Parra, pers. comm., 2011). No or very little vegetation surrounds these lakes. The glacial nature of these deposits is confirmed by ages close to 17,000 cal yr BP obtained in the uppermost part of the unit (Fig. 5). Unit 1 corresponds to the late Pleniglacial (Fig. 5).

The limit between units 1 and 2 is marked by an unconformity corresponding to a major palaeoenvironmental change. The organo-mineral Unit 2 without vegetal fibres can be interpreted as an environment of a few-metre deep páramo black lakes (Parra et al., 2010c). This unit contains mineral mud associated to the deglaciation and mixed with organic matter from the growing vegetation. Unit 2 contains at its base several tephra levels tentatively correlated by Parra et al. (2010d) with the eruptive stages called Canalones and Romerales by Thouret et al. (1995). According to the age model (Fig. 5) they are dated between 15,000 and 17,000 cal yr BP. Unit 2 corresponds to the Lateglacial, with its upper part being equivalent to the YD (Fig. 5).

Unit 3 corresponds to the Holocene period during which the LLG depression was infilled mainly by vegetal fragments and little minerals. It was covered by marshes, peat bogs and very shallow, brackish páramo black lakes (Parra et al., 2010c). The thin tephra layer encountered in cores LLG-2 to −9 at a depth of ca. 4 m (isochron a, Figs. 4 and 5) has been previously interpreted as the "Salamina" tephra related to the eruption of the Cerro Bravo volcano and dated at between 6500 and 7200 yr BP (Parra, 1991; Parra et al., 2010b), i.e., 7400–8000 cal yr BP. According to the age model obtained in LLG (Fig. 5), this ash layer appears younger with an age of ca. 6000 cal yr BP.

Apart from the limit between the glacial clays of the late Pleniglacial and the onset of the organic-rich sedimentation in the Lateglacial (Fig. 4), the whole Lateglacial and Holocene sequence in cores LLG-2 to −9 does not present any indication of unconformities or significant hiatuses in the sedimentation. The 30 AMS ^{14}C datings obtained throughout this sequence confirm the remarkable continuity of the deposition (Fig. 5).

5.2. Environmental reconstruction

In this section we present a reconstruction of the Holocene climatic variability in LLG, which can be inferred from the biotic (arboreal and aquatic pollen) and abiotic (μXRF) proxies.

Time series analysis has been carried out on the ultra-high (subannual) resolution μXRF data. The Morlet wavelet spectrum (MWS) has been analyzed over the interval 12,000 - 0 cal yr BP both for Ti and Fe and can be studied with respect to the palynological and geochemical precipitation proxies (Fig. 6 and Suppl. Fig. 2). The MWS permits the identification of changes in variance through time within selected frequency time bands. Yellow to red areas indicate a high degree of variance, and a black line surrounds regions of variance that exceed the 95% confidence level for a red noise process (at 4–16 yr period, the regions of significant variance are shown black rather than outlined). The MWS of Ti (Fig. 6) shows a high degree of cyclicity for phenomena in the millennial bands throughout the late YD and Holocene, whereas a high activity in the 500 yr down to sub-decadal (i.e., ENSO) bands is restricted to more specific time intervals.

The Holocene record in Frontino is marked by rapid and significant changes in temperature and precipitation. Temperatures may have varied a few degrees centigrade over less than a century and changes in rainfall were either progressive or abrupt (Fig. 6). All proxies show that the upper part of the YD (*interval 1*) was cold and wet. Between 12,000 and 11,410 cal yr BP, the MWS of Ti displays a high variance from the millennial bands down to the ENSO band. The base of the Holocene (*interval 2,* 11,410–10,700 cal yr BP) was warm and dry and the MWS does not show much variance in the centennial to ENSO bands. Cold and dry conditions prevailed in *interval 3* (10,700–9700 cal yr BP) with some occasional high variance in the high frequencies (e.g., ENSO band). *Interval 4* (9700–6900 cal yr BP) was overall warm and can be interpreted as the "Holocene thermal maximum" (e.g., Haug et al., 2001; Niemann et al., 2009; Renssen et al., 2009, 2012; Wanner et al., 2014). It was interrupted by a colder break at around 8000 cal yr BP (Fig. 6), which might be an expression of the 8.2 ka event well known in the North Atlantic (e.g., Alley and Ágústsdóttir, 2005; Rohling and Palike, 2005; Cheng et al., 2009). The small offset in time might be due to inaccuracy of the age model or correspond to a real lag time associated with the response of the tropics to this event. Interval 4 was overall dry until ca. 7500 cal yr BP (low Ti signal and low estimated water level in the mire). Some slightly wetter intervals might occur (visible in the Ti signal) and the MWS shows occasional high variance in the centennial to ENSO bands. The period 7700–7500 cal yr BP is very dry and marked by dessiccation in the mire. This period coincides with a very low activity in the 500 yr to sub-decadal bands of the MWS. The following period between 7500 and 4200 cal yr BP is the wettest of the Holocene and coincides with a climate colder than today between 7000 and 4200 cal yr BP. The Ti signal highlights three rainfall maxima, between 7500 and 7000, 5600 and 5300 and 5000 and 4200 cal yr BP. These maxima coincide with a high variability in the 500 yr to subdecadal bands of the MWS. The first peak in rainfall (7500–7000 cal yr BP) coincides with the decrease and near-disappearance of the driest aquatic vegetation in the mire (Fig. 6). The second and third peaks in rainfall are matched by an increase in the estimated water depth of the mire, which reaches a maximum between 5000 and 4200 cal yr BP. In the uppermost part of interval 5 (from about 4200 cal yr BP), rainfall inferred from Ti (and Fe, Fig. 6 and Suppl. Fig. 2) starts decreasing and continues to decrease rapidly in *interval 6* (4000–2400 cal yr BP) to reach a minimum between ca. 2800 and 2600 cal yr BP, when it coincides with a maximum in temperature. This decrease in rainfall inferred from the geochemical proxies (Ti and Fe) matches well the water level of the mire derived from local aquatic plants (Fig. 6). The rapid decrease in rainfall in interval 6 coincides with a decrease in activity in the 500 yr to ENSO bands of the MWS. At ca. 2400 cal yr BP the UFL drops suddenly and remains low during most of *interval 7* (2400-0 cal yr BP). Although this abrupt drop is probably climate-forced, the AP% cannot be used as a temperature proxy in interval 7 because of human impact (Flantua et al., 2016a): anthropogenic deforestation during the last 2.3 kyr around the Páramo de Frontino is supported by the rapid decrease in *Quercus* and the significant increase in asteraceous shrub and grasses as a consequence (Velásquez, 2005). Nevertheless, the rapid increase in AP% over the last 200 years demonstrates a significant warming over this period (well-known from ice core records in tropical South America (SA) (Thompson et al., 1995, 2000) and from pollen records in northern Ecuador (Bakker et al., 2008; Moscol Olivera and Hooghiemstra, 2010)). This implies that the MAT, although it cannot be directly inferred from the AP% because of human impact, was lower than today for most of the last 2 kyr. During the last 2000 years, sedimentation in the LLG mire corresponds essentially to peat formation with very little mineral influx (extremely low Ti and low Fe signals). This points to overall dry conditions, but minor wetter phases can be detected in the Fe signal, which increases in intensity between ca. 2500 and 500 cal yr BP (Fig. 6 and Suppl. Fig. 2). The aquatic plants also show an increase in the estimated water depth, especially between 1700 and 900 cal yr BP.

6. Discussion

6.1. Local climate

In this section, we discuss the relevance of our multiproxy approach to reconstruct the humidity/rainfall record of the YD and Holocene. We also discuss the contribution of time series analysis of μXRF data to the interpretation of climate mechanisms. Finally, we demonstrate the importance of testing the LLG sedimentary record in its optimal location with an accurate age model.

The contribution of multiproxy tools in palaeoenvironmental reconstruction has been emphasized by Flantua et al. (2015). In our study we base the reconstruction of humidity/rainfall on a biotic (aquatic pollen) and abiotic (μXRF) proxy and can assess their (dis) advantages. μXRF measures the amount of chemical elements (in minerals) brought in the basin by runoff waters. Therefore, this signal gives a precise "instantaneous" indication of the amount of rainfall in the catchment area. By contrast, the local aquatic vegetation gives only an estimation of the water depth in the mire with a time lag of an estimated decade minimally. Moreover, the two proxies have a different temporal resolution: the pollen record between 20 and 35 yr, and μXRF a sub-annual resolution. The latter is consequently more accurate and quite suited for time series analysis. Finally, these two proxies are derived from two different cores and there might be some offset between records because of the age model. The visual comparison between the high-resolution μXRF Ti curve and the water depth estimated from aquatic plants shows an overall similarity (Fig. 6). In the YD, high rainfall coincides with a significant water depth in the mire. Between 11,410 and 7500 cal yr BP, reduced rainfall coincides with a low water level in the mire. During this period, the short peaks in rainfall observed in μXRF data are not registered in the aquatic pollen record. Between 7500 and 4200 cal yr BP, the increase in rainfall inferred from Ti and Fe is matched by an increase in the estimated water depth of the mire, which reaches a maximum between 5000 and 4200 cal yr BP. The rapid decrease in rainfall between 4200 and 2600 cal yr BP coincides with a lowering water level in the mire. During the last 2600 years the comparison between the two proxies is difficult because of the very low influx of minerals in the mire. This comparison of proxies demonstrates that aquatic pollen-based records of past lake-level changes can provide a valuable means to assess precipitation (Van Boxel et al., 2014; Urrego et al., 2016), although they yield less precise results than high-resolution μXRF.

The MWS of Ti and Fe (Fig. 6, Suppl. Fig. 2) shows a wide spectrum of frequencies in the precipitation regime from millennial to annual scales. A high variance in the millennial bands exists throughout the record. Millennial-scale climate variability in the Holocene is commonly attributed to solar variability. Of all potential climate-forcing mechanisms, Mayewski et al. (2004) consider solar variability superimposed on long-term changes in insolation as most likely the important forcing mechanism for rapid climate change in the Holocene. Most statistical analyses find significant correlations between regional South American precipitation and Pacific sea-surface temperatures (SSTs) (Cook, 2009), and millennial-scale fluctuations in SSTs correlate with cosmogenic nuclide proxies of solar variations (Marchitto et al., 2010). Redistribution of solar energy due to orbital forcing on a millennial timescale is the inferred cause of the progressive southward shift of the ITCZ during the last 6000 years (Wanner et al., 2008). High variance at multi-centennial to decadal timescales occurs in LLG during specific time intervals from the YD till ca. 3000 cal yr BP (Fig. 6, Suppl. Fig. 2). Multi-centennial cycles during the Holocene in the Peruvian Andes are attributed to solar variations (Bush et al., 2005). Decadal to centennial dry-wet oscillations at the Lateglacial-Holocene transition in the Central Andes could have been triggered by both solar and ENSO activity (Hernández et al., 2010). Recent climate model studies suggest that even low amplitude solar variations can affect climate on multi-decadal to centennial timescales (Ammann et al., 2007). Finally, the precipitation regime in LLG seems to be directly related to the activity of ENSO: the high variance in the 4–8 yr ENSO band coincides with the intervals of high rainfall interpreted from μXRF or aquatic plants.

Velásquez and Hooghiemstra (2013) published the pollen record of core LLG-1. The age model of this 17 kyr long record relies on only six ^{14}C dates. Unfortunately, this core is located on the flank of the basin (Fig. 2C) and penetrated a condensed sedimentary section with hiatuses (Fig. 4). Consequently, it is difficult to establish a correlation with data used in the present study, which originate from the well-dated, hiatus-free, deepest part of the basin (cores LLG-2 and -5). The sharp transition between the YD and the Holocene at 11,410 cal yr BP in LLG-2 is the only precise correlation point that can be established with core LLG-1, where a similar change from a cold and wet YD to a warm and dry basal Holocene is observed at a depth of ca. 565 cm (Velásquez and Hooghiemstra, 2013). Finally, the importance of sampling a hiatus-free, stratigraphically continuous section (Van 't Veer et al., 2000; Groot et al., 2013) is perfectly illustrated by the following observation: in LLG-1, the first indication of human impact (deforestation of *Quercus*, *Podocarpus* and *Weinmannia* and increase in asteraceous shrub and grasses) is interpreted at ca. 620 cal yr BP, whereas in the centre of the basin human impact is shown by the rapid decrease in *Quercus* and the significant increase in asteraceous shrub and grasses (Velásquez, 2005) since ca. 2300 cal yr BP!

6.2. Regional correlations

The LLG record shows the first Holocene multiproxy record in the neotropics at a near-decadal to sub-annual scale (Flantua et al., 2015). With such a resolution one might try to distinguish purely local variations from a more regional signal. In this section, we present a comparison of Frontino data with selected northern South American palaeoclimatic records (Fig. 7) of Lateglacial and Holocene times to attempt a better understanding at the regional scale.

Regional correlations face several problems. The topography of the Andes plays an important role, in particular when analyzing humidity records (Urrego et al., 2016). Moreover, the quality and accuracy of the data differ considerably from one record to another, as well as the precision of the age model (Flantua et al., 2016b). Except for the marine Cariaco Basin in the Venezuelan Caribbean Sea (Haug et al., 2001; Lea et al., 2003; Petersen and Haug, 2006), selected comparison sites are high-altitude locations distributed along a N-S Andes transect (Fig. 1). Temperature and humidity data at these sites are derived essentially from pollen records, except for the humidity data in the Laguna Los Anteojos (Venezuela, Stansell et al., 2010) and Laguna Rabadilla de Vaca (Equator, Niemann et al., 2009) where humidity information originates from Ti XRF records, and in the Huascaran ice core (Peru, Thompson et al., 1995) where temperature data come from oxygen isotope ratio $\delta^{18}O$ measurements. All pollen records have an over 100 yr resolution, except for record La Cocha in Colombia (González-Carranza et al., 2012) with a 25 yr resolution. The Cariaco site is of particular interest because of its XRF data with a 5 yr resolution (Haug et al., 2001; Petersen and Haug, 2006), which provide the best precipitation proxy in the coastal Venezuelian cordilleras for correlation with Frontino. Moreover, Cariaco is located in the Atlantic (Caribbean Sea) and its latitudinal position is close to that of Frontino, making it a very valuable correlation point to try to distinguish Atlantic vs. Pacific-driven climatic influence. Both sites are located in the narrow band of low-level wind convergence over the equatorial oceans where the seasonal migration of the ITCZ primarily affects coastal areas and northernmost SA (Flantua et al., 2016a). A detailed comparison between the two sites will be discussed separately in the next section.

The rapid increase in temperature at ca. 11,410 yr BP in LLG (Fig. 6) is interpreted as reflecting the termination of the South American equivalent of the YD cool period, referred to as the « El Abra stadial » in Colombia (Van der Hammen and Hooghiemstra, 1995; Van 't Veer et al., 2000). The explanation for this abrupt global temperature shift favours either tropical (Clement et al., 2001) or high latitude (Broecker, 2006) ocean-atmosphere systems as the dominant driving mechanisms. Whatever the initial cause of the YD, the tropics must have played an important role in modulating the climate system during and at the termination of the event (Stansell et al., 2010). In the Northern Hemisphere, the YD

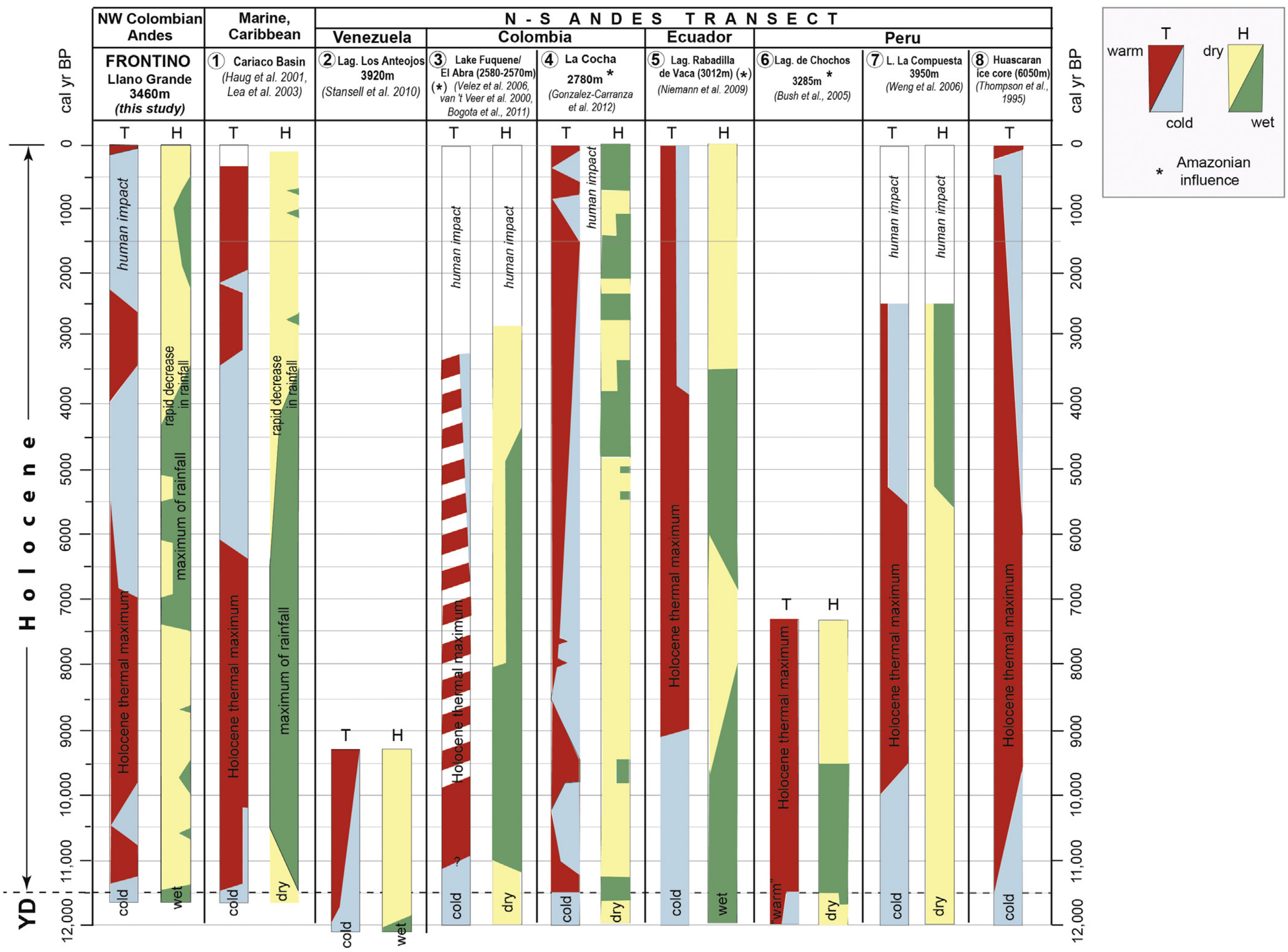

Fig. 7. Palaeoennvironmental reconstruction in the Páramo de Frontino compared with other selected pollen and one ice core records in the northern and central Andes (see site location in Fig. 1). Comparison of proxy-derived temperature (T) and humidity (H) data.

cold reversal occurs between about 12,850 and 11,650 cal yr BP (Rasmusen et al., 2006). In Frontino, the end of the YD is dated at ca. 11,410 cal yr BP. In tropical Central and South America, the YD cold period is observed at several sites, but precise datings in non-condensed sections are lacking and its upper boundary is still insufficiently known (Van der Hammen and Hooghiemstra, 1995; Van 't Veer et al., 2000). In this respect, Frontino provides a new high-resolution data point for precisely dating the end of the YD in this region.

The YD is observed in the Caribbean area (Cariaco) and in selected sites in the Andes as far south as Peru (Fig. 7). It is normally registered as a dry period, except in the high-altitude sites of Frontino in Colombia and Laguna Los Anteojos in the Mérida Andes of Venezuela in the north, and of Laguna Rabadilla de Vaca and Laguna Pallcacocha/Chorreras (Hansen et al., 2003) in southern Ecuador. There is a striking difference between Frontino and Cariaco where XRF data show respectively a very wet and a very dry YD (Fig. 8).

During the period of 11,500–8000 cal yr BP, most of the sites show an increase in temperature (Fig. 7). This is interpreted by the authors as the “Holocene thermal maximum” (e.g., Haug et al., 2001; Renssen et al., 2012; Wanner et al., 2014). In Frontino and Cariaco, the overall increase is significant right from the beginning of the Holocene, whereas the onset of this warming may occur later or be more gradual or irregular in the other sites. Humidity records are more contrasted and depend highly of the geographical location. The most striking feature is observed between Frontino, the Laguna Los Anteojos (Mérida Andes) and Cariaco, where Ti XRF data are available: at the first two locations conditions become dry, whereas, by contrast, the Caribbean area becomes gradually wetter (Fig. 7). Similarly to Cariaco, other sites in Central America show wet conditions at the beginning of the Holocene, e.g., in Panama (Piperno and Jones, 2003) and Costa Rica (Islebe et al., 1995). This results from the northward migration of the ITCZ after the YD (Haug et al., 2001). The dry conditions in Frontino (and possibly the Mérida Andes) may be Pacific-driven and related to the low activity of ENSO (Fig. 6). Other sites further south (Fig. 7) in Colombia (Lake Fúquene in the Eastern Cordillera), Ecuador (Laguna Rabadilla de Vaca) and Peru (Laguna de Chochos) show wetter conditions possibly related to moisture supply by trans-Amazonian air flows (Fu et al., 2001; Vizy and Cook, 2007).

During the period of 8000–4000 cal yr BP, most of the records in Colombia, Venezuela, Ecuador and Peru (Fig. 7) show a temperature decrease at some stage, which is interpreted as the end of the “Holocene thermal maximum” (Frontino, Mérida Andes, Cariaco, Rabadilla de Vaca, Lago la Compuesta, Huascaran Glacier). Both Frontino and Cariaco show a significant cooling between 6000 and 4000 cal yr BP. Humidity variations are more difficult to compare, because the accuracy of the proxy used differs considerably. An overall decrease in precipitation is observed in Cariaco between

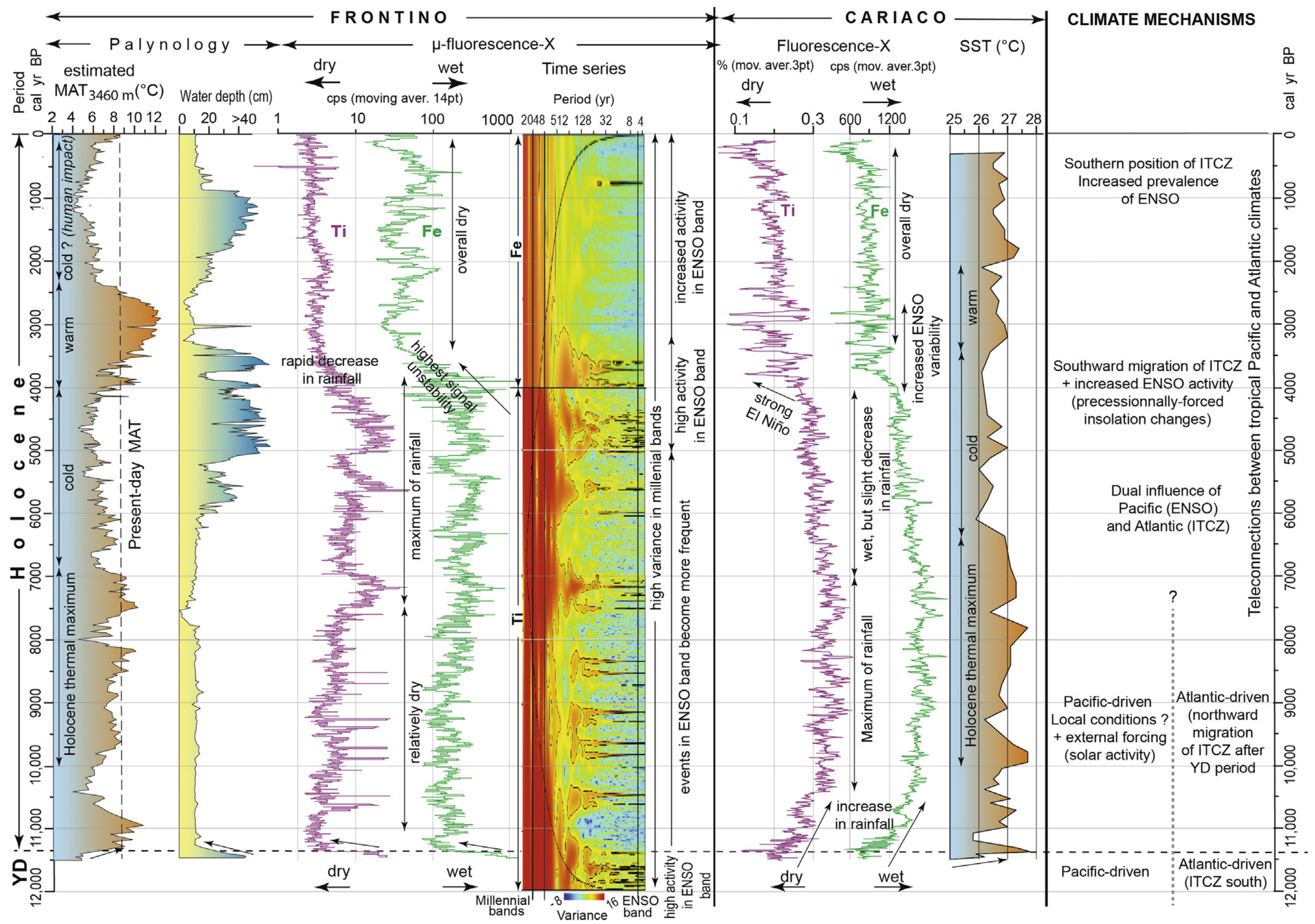

Fig. 8. Comparison of temperature and precipitation data derived from several biotic and abiotic proxies in the Páramo de Frontino and the marine Cariaco Basin in Venezuela. Implications for regional climate mechanisms. Cariaco data are derived from Haug et al. (2001) for X-ray fluorescence and from Lea et al. (2003) for sea surface temperature (SST).

7000 and 4000 cal yr BP. A similar decrease in moisture is also registered in the Mérida Andes of Venezuela (Laguna Verde Alta, Rull et al., 2005) and in Central America in Costa Rica (Islebe et al., 1995) and the Yucatan Peninsula (Carrillo-Bastos et al., 2010). This is interpreted as resulting from the southward migration of the ITCZ (Haug et al., 2001). By contrast, Frontino shows an overall increase in precipitations with a maximum between ca. 5000 and 4500 cal yr BP coinciding with an increased activity of ENSO (Fig. 6). In the Laguna Rabadilla de Vaca (southern Ecuador), the maximum of precipitations occurs between 6000 and 3500 cal yr BP (Fig. 7). This could also be the effect of increased ENSO activity, or humidity supply from the Amazon. East of the Colombian Andes in the lowlands, the period of 8000–4000 cal yr BP is marked by alternations of wet and dry periods, maybe becoming wetter towards the top (Behling and Hooghiemstra, 2000; Vélez et al., 2006).

The palaeoclimatic reconstruction of the period of 4000–0 cal yr BP in Frontino has been derived from pollen record by Velásquez (2005). It is complemented here with new µXRF data and related statistics (Fig. 6 and Suppl. Fig. 2). With respect to temperature, the model based on the AP% in Frontino shows a significant period of warming between 4000 and 2500 cal yr BP. This temperature increase is accompanied by dry conditions (Fig. 6). This increase is difficult to confirm in the Colombian Andes because of lack of high-resolution records (Flantua et al., 2015), except in the south, in Lake La Cocha, where warm conditions seem to prevail until 1500 cal yr BP (Fig. 7) and in the Eastern Cordillera where warm conditions lasted at least until 3.2 kyr (Fúquene-2, Bogotá-Angel et al., 2011). In southern Ecuador (Lag. Rabadilla de Vaca) and in Peru (Lago La Compuesta, Huascaran Glacier), the late Holocene is interpreted as a cold period (Fig. 7). After 2400 cal yr BP, temperatures in Frontino drop rapidly, but MAT cannot be estimated because of the human impact (deforestation) observed from ca. 2300 cal yr BP (Fig. 6). Temperature increases rapidly over the last 200 years (Fig. 7), as also observed in southern Colombia (La Cocha) and Peru (Huascaran glacier). Humidity data show overall dry conditions in Frontino, with some oscillations observed in µXRF (Fe data) and pollen data (Fig. 6). Similarly, overall dry conditions in the late Holocene are also registered in Cariaco and Central America (Costa Rica and Yucatan peninsula). This is related to the southern position of the ITCZ (Haug et al., 2001).

Therefore, although the quality of the data is disparate, these regional correlations tend to highlight the influence of at least three mechanisms that have been proposed to explain Holocene climate variability in northern SA: the northward/southward migration of the ITCZ, the varying activity of ENSO and the humidity supply by trans-Amazonian air flows.

6.3. Correlation with the Cariaco Basin and implications for regional climate mechanisms

In this section, we focus on the high-resolution data of Frontino and Cariaco, in order to better understand the climate mechanisms that affected these areas and the potential connections between Pacific and Atlantic climates during the Holocene (Fig. 8).

In tropical northern SA, oceanic-atmospheric systems regulate present-day and past climatic variations. The most important system is the Atlantic ITCZ driven by high latitude forcing in the northern Atlantic. Changes in its mean position best explain precipitation variation (Petersen and Haug, 2006; Flantua et al., 2016a). This high-latitude Atlantic-driven forcing mechanism interacts with another oceanic-atmospheric system characterizing the tropical Pacific, i.e., the ENSO (Vuille and Werner, 2005; Vuille and Garreaud, 2012). In the Colombian Andes during the last 2000 years, more than two thirds of the temperature variability on interannual scales can be explained by ENSO, which also leads to the strongest modern precipitation anomalies (Flantua et al., 2016a). These two mechanisms are today the best explanations for the large and abrupt climate changes characterizing the Late-glacial and Holocene in northernmost SA. Both mechanisms are important, but the degree to which each contributes is timescale dependent and there is a need for more high-resolution palaeoclimatic records in areas exposed to ITCZ and ENSO influences (Petersen and Haug, 2006).

In this respect, the LLG record is ideally located because Frontino is exposed to the influence of both oceans. It is so far the only high-altitude, high-resolution, multiproxy record in the Western Cordillera of Colombia (Flantua et al., 2015). Because of its high-resolution (5 yr) XRF data, the Cariaco Basin remains the best comparison point as rainfall proxy (Fig. 8) in northern SA. Moreover, SST in the tropical Atlantic (Lea et al., 2003) can be used as comparison for temperature variations (although with a resolution of only 200 yr).

As far as temperature is concerned, the interpretation obtained from pollen record in Frontino fits the overall picture known in this region. A cold YD equivalent (El Abra stadial in Colombia, Van der Hammen and Hooghiemstra, 1995; Van 't Veer et al., 2000) is present, with an estimated MAT some 3.5 °C lower than today. This figure can be compared with that of ca. 5 °C in the Eastern Cordillera of Colombia (Groot et al., 2011), of 3 °C suggested by Van 't Veer et al. (2000) for Costa Rica, Guatemala and Colombia, and that of 2.2–2.9 °C in the Venezuelan Andes (Stansell et al., 2010). An abrupt increase in temperature marks the base of the Holocene in Frontino, similarly to that observed in SST of Cariaco (Fig. 8). An interval of overall higher temperatures straddles the period of ca. 10,000 till 6500 cal yr BP in Frontino and can be referred to as the « Holocene thermal maximum ». It is also well expressed and synchronous in Cariaco (Fig. 8). It is encountered in most of the sites used for comparison (Fig. 7), although its actual onset and duration seem to vary from site to site (because of location, local climatic conditions, time resolution and accuracy of age model). The period of 6000–4000 cal yr BP in Frontino becomes considerably colder with MAT possibly 2.5 °C lower than today. This cold period coincides with a cold interval observed from SST in the Caribbean (Fig. 8). In the upper part of the Holocene, the temperature model of LLG (Fig. 8) suggests a temperature maximum culminating at ca. 3000 cal yr BP. In Cariaco, SST also shows a high at around 3000 cal yr BP. From ca. 2400 cal yr BP, colder conditions probably prevailed in Frontino, but cannot be properly estimated because of human impact (deforestation) after 2300 cal yr BP (Fig. 8). Cold conditions are also encountered during the last 3000 years in Ecuador (Laguna Rabadilla de Vaca and in core G15-II in northern Ecuador, Bakker et al., 2008) and Peru (Huascaran ice core, Fig. 7). In the Carribean Sea warm conditions prevailed during the last 2000 years (Fig. 8).

μXRF data in Frontino (supported by the aquatic pollen proxy, Fig. 8) show a very abrupt change from a wet YD to a much drier Holocene. By contrast, XRF data in Cariaco show the opposite (Haug et al., 2001; Petersen and Haug, 2006): the YD is dry and the transition to a wet Holocene is progressive (Figs. 7 and 8). Similarly, in the Yucatan Peninsula (Lake Peten Itza), Hodell et al. (2008) observe a dry YD followed by the return to wetter conditions in the early Holocene. Both in Cariaco and Yucatan (Caribbean Sea), authors explain the dry conditions of the YD through the latitudinal displacement towards the south of the mean position of the ITCZ during the last glacial maximum. With the warming phase at the base of the Holocene, the ITCZ migrated northwards, resulting in progressively wetter conditions at both sites. The latitudinal position of Frontino is close to that of the coastal Venezuelian cordilleras draining into the Cariaco Basin (Fig. 1). If Frontino precipitation regime at the YD-Holocene transition had been directly influenced by the ITCZ, one would expect a similar signal to that encountered in Cariaco (similarly to what happens during the period of 4500–3500 cal yr BP, see below). Moreover, the abrupt YD-Holocene change in precipitation in Frontino looks quite different from the gradual transition observed between 4500 and 3500 cal yr BP (Fig. 8). Therefore, we postulate that the moisture regime in the YD and early Holocene in Frontino might have been more under the influence of the Pacific Ocean (ENSO, Choco Jet) than under that of the Atlantic Ocean (influence of ITCZ dominant in the Caribbean Sea). The MWS of Ti in Frontino (Figs. 6 and 8) shows high variance in the ENSO band for the last 600 years of the YD. In the early Holocene, all high frequencies decrease in variance, with only some short events affecting the ENSO band. Moreover, high variance in the millennial bands is observed in Frontino during the late YD and early Holocene (Fig. 8). This could be related to the influence of solar forcing with millennial-scale fluctuations, as demonstrated in the Pacific Ocean during the early Holocene (Marchitto et al., 2010).

Cariaco and Frontino exhibit contrasting rainfall patterns between 11,400 and 4000 cal yr BP (Fig. 8). In Cariaco, increasing rainfall in the early Holocene is followed by a precipitation maximum coinciding with the Holocene thermal maximum between ca. 10,000 and 7000 cal yr BP. This is consistent with the postulated northward migration of the ITCZ after the YD. The correlation of this wet and warm interval in Cariaco with La Niña-like wet conditions in the eastern equatorial Pacific (Marchitto et al., 2010) is an argument to interpret the existence of already existing ENSO teleconnections at that time (Stott et al., 2002). From 7000 cal yr BP, precipitations in Cariaco start to decrease slightly until 4000 cal yr BP and drop rapidly afterwards (Fig. 8). This is interpreted as reflecting the southward migration of the ITCZ leading to dry conditions in the late Holocene. The picture in Frontino is different. μXRF data (supported by aquatic pollen proxy, Fig. 8) show an overall increase in precipitation between 11,400 and 4500 cal yr BP with a maximum centered over 5000–4500 cal yr BP. Superimposed on this general trend, both Ti and Fe data show oscillations at millennial and sub-millennial timescales (Fig. 8). The MWS of Ti displays continuous high variance in the millennial bands during this period (Figs. 6 and 8). In the ENSO band, intervals of high activity are very intermittent but increase in frequency, particularly between 7500 and 4000 cal yr BP. We interpret these data as reflecting the dual signature of the ITCZ and ENSO: the overall increase in rainfall would be the result of the southward migration of the ITCZ, whereas the higher frequency cycles would be linked to ENSO. These observations in Frontino can be compared with those of Moy et al. (2002), who have interpreted in the Laguna Pallcacocha in Ecuador that warm ENSO events became more frequent throughout the Holocene, with a superimposed trend showing periods of high and low ENSO activity at timescales of 2000 years. Orbitally-driven external forcing with a 1000/2500 yr cyclicity (Debret et al., 2009; Marchitto et al., 2010) may also be an important factor. The influence of ENSO variability after 7000 cal yr

BP has also been recognized in Lake La Cocha in the southern Colombian Andes (González-Carranza et al., 2012).

The rainfall record in Cariaco and Frontino over the last 5000 years highlights the dual influence of ITCZ and ENSO over the climate in both areas (Fig. 8). The XRF record in Cariaco illustrates the rapid change towards dry conditions after ca. 3000 cal yr BP. This decrease in rainfall was associated with the southward shift of the ITCZ (Haug et al., 2001; Petersen and Haug, 2006) and coincided with an increase in ENSO activity. The latter was probably related to a precessional control (Clement, 1999; Clement et al., 2001), leading to the prevalence of dry El Niño events in the late Holocene. In lake sediments from Ecuador, Rodbell et al. (1999) showed that modern ENSO periodicities were established only after about 5 ka. Haug et al. (2001) have related these observations to precessionally-forced insolation changes. The latter would have directly forced the southward migration of the ITCZ, but also increased the prevalence of El Niño through the Holocene. This would have further amplified the southward shift of the ITCZ while adding a higher frequency component to its latitudinal variations. The MWS in LLG indicates that between 5100 and 4300 cal yr BP both Ti and Fe signals show the highest variance of the whole Holocene in the high frequency bands (e.g., ENSO), which coincides with the maximum of rainfall (Suppl. Fig. 2 and Fig. 8). Between 4300 and 3500 cal yr BP, the significant decrease in rainfall in both areas results from the southward migration of the ITCZ, but also coincides with a strong ENSO variability (Fig. 8, Haug et al., 2001). Between 3500 and 260 cal yr BP, although the Fe signal is very stable in variance, it is only perturbed by frequent short events in the ENSO band.

Therefore, comparison of rainfall between Frontino and Cariaco suggests that climate in the northern part of the Western Cordillera was probably Pacific-driven in the YD and early Holocene with little influence of the Atlantic-driven ITCZ. From ca. 8000 cal yr BP, both areas seem to be under the dual influence of ENSO and ITCZ, which highlights the existing teleconnections between tropical Pacific and Atlantic climate (Fig. 8).

7. Conclusions

We have analyzed the stratigraphically continuous sedimentary archive of the LLG mire in the northernmost part of the Colombian Western Cordillera using two proxies, which permitted the study of the biotic (pollen) and abiotic (μXRF) components of this high-mountain ecosystem. The time interval studied covers the last 11,500 cal yr BP and comprises the uppermost YD and the Holocene. The studied interval is accurately dated by a robust age model. The ultra-high resolution of the results (20–35 yr for pollen, ca. 6-months for the μXRF) makes this record unique for the study of Holocene climate variability in northwesternmost SA, where climate dynamics is essentially governed by the interaction between oceanic-atmospheric systems of the ENSO and ITCZ.

We have demonstrated the important climate variability in Frontino at various timescales (Fig. 6). The transition from the YD to the Holocene was very rapid and is accurately dated at 11,410 cal yr BP. Throughout the Holocene, estimated MAT varied from 2.5 °C lower up to 3.5 °C higher than today with an alternation of warm and cold periods. The last 2400 years were probably colder than today, but human impact affects the pollen record from 2300 cal yr BP. We have reconstructed the precipitation regime using both pollen and μXRF data. The latter have been analyzed by spectral analysis, which shows rainfall periodicities in the millennial bands throughout the Holocene, whereas centennial down to ENSO band periodicities are observed in more specific intervals, which coincide with increased precipitation (Fig. 6). Correlations with other selected sites in tropical northwestern SA have confirmed that ITCZ (Atlantic-driven) and ENSO (Pacific-driven) are the main mechanisms influencing the climate in this area. We have used the marine Cariaco Basin in Venezuela as the best reference correlation site, because of its high-resolution XRF data and its location in the Atlantic climate realm. The influence of ENSO and ITCZ varied over time in the two locations, with an additional external forcing due to solar radiation which influences periodicities from millennial down to decennial time scales. During the YD and early Holocene, we have interpreted the climate in Frontino as Pacific-driven (strong influence of ENSO) and that in Cariaco as Atlantic-driven (dominated by the position of ITCZ). From ca. 8000 cal yr BP until now, both areas show the dual influence of ITCZ and ENSO and the existing teleconnections between Pacific and Atlantic oceans climate (Fig. 8).

We have compared the humidity record of aquatic plants with the rainfall proxy provided by μXRF of Ti and Fe (Fig. 6). Because of its sub-annual resolution, μXRF is much more precise, but overall it correlates well with the aquatic pollen information. This demonstrates that climate reconstructions from pollen record should not only focus on temperature, but also include information about precipitation, which is an equally important parameter (Van Boxel et al., 2014). Our study has illustrated the value of multiproxy-based research in palaeoclimatic investigations (Flantua et al., 2016a). We have demonstrated the value of ultra-high resolution μXRF and advocate its use as rainfall proxy in future multiproxy studies. It provides high-resolution time series that can be explored with frequency analysis and provide support for climate-driving mechanisms (Flantua et al., 2016a). Ongoing research (Monsalve, 2015) aims at testing in Frontino the same multiproxy high-resolution approach on the Lateglacial interval from 17,000 till 11,500 cal yr BP. Once completed, this Lateglacial study will be coupled with our present Holocene data and provide the most accurate, stratigraphically continuous record of the last 17 kyr in NW Colombia. The continuous sedimentary sequence in LLG should also be investigated by other biotic climate proxies, such as diatoms and chironomids. Finally, similar multiproxy investigations should be undertaken on lower altitude sites in the Western Cordillera of Colombia.

Acknowledgements

The authors are indebted to the authorities of the Parque Nacional Natural las Orquídeas for their help in facilitating the various field campaigns to the Páramo de Frontino. PM thanks the Palaeoecology Laboratory of the National University of Colombia in Medellín and the Institute for Biodiversity and Ecosystem Dynamics (IBED) of the University of Amsterdam (Holland) for the use of their palynological reference collections. GG thanks Gerald Haug for providing the Ti and Fe data from the Cariaco Basin. All authors are extremely grateful to Henry Hooghiemstra for his extensive review of a former version of this manuscript. They also thank Valenti Rull for his comments. This research has been supported by the Swiss National Science Foundation (grant no. 200020-112320).

Appendix A. Supplementary data

Supplementary data related to this article can be found at http://dx.doi.org/10.1016/j.quascirev.2016.11.021.

References

Alley, R.B., Ágústsdóttir, A.M., 2005. The 8k event: cause and consequences of a major Holocene abrupt climate change. Quat. Sci. Rev. 24, 1123–1149.
Ammann, C.M., Joos, F., Schimel, D.S., Otto-Blisner, B.L., Tomas, R.A., 2007. Solar influence on climate during the past millennium: results from transient simulations with the NCAR climate system model. Proc. Natl. Acad. Sci. U. S. A. 104,

3713–3718.

Bakker, J., Moscol Olivera, M., Hooghiemstra, H., 2008. Holocene environmental change at the upper forest line in northern Ecuador. Holocene 18, 877–893.

Behling, H., Hooghiemstra, H., 2000. Holocene Amazon rainforest–savana dynamics and climatic implications: high-resolution pollen record from Laguna Loma Linda in eastern Colombia. J. Quat. Sci. 15, 687–695.

Bogotá-Angel, R.G., 2011. Pleistocene Centennial-scale Vegetational, Environmental and Climatic Change in the Colombian Andes: Based on Biotic and Abiotic Proxy Analyzes from Lake Fúquene Sediments. Ph D Thesis. Institute for Biodiversity and Ecosytems Dynamic (IBED). University of Amsterdam, 144 pp.

Bogotá-Angel, R.G., Groot, M.H.M., Hooghiemstra, H., Lourens, L.J., Van der Linden, M., Berrio, J.C., 2011. Rapid climate change from north Andean Lake Fúquene pollen records driven by obliquity: implications for a basin-wide biostratigraphic zonation. Quat. Sci. Rev. 30, 3321–3337.

Boom, A., Marchant, R., Hooghiemstra, H., Sinninghe Damsté, J.S., 2002. CO2- and temperature controlled altitudinal shifts of C4- and C3-dominated grasslands allow reconstruction of paleoatmospheric pCO2. Palaeogeogr. Palaeoclimatol. Palaeoecol. 177, 151–168.

Bradbury, J.P., Leyden, M., Salgado-Labouriau, M., Lewis, W.M., Schubert, C., Binford, M.W., Frey, D.G., Whitebread, D.R., Weibezahn, F.H., 1981. Late quaternary environmental history of lake Valencia, Venezuela. Science 214, 1299–1305.

Broecker, W.S., 2006. Was the younger Dryas triggered by a flood? Science 312, 1146–1148.

Brunschön, C., Behling, H., 2010. Reconstruction and vizualisation of upper forest line and vegetation changes in the Andean depression region of southeastern Ecuador since the last glacial maximum – a multi-site analysis. Rev. Palaeobot. Palynol. 163, 139–153.

Bush, M.B., Hansen, B.C.S., Rodbell, D.T., Seltzer, G.O., Young, K.R., Leon, B., Abbott, M.B., Silman, M.R., Gosling, W.D., 2005. A 17.000-yr history of Andean climate and vegetation change from Laguna de Chochos, Peru. J. Quat. Sci. 20, 703–714.

Carrillo-Bastos, A., Islebe, G.A., Torrescano-Valle, N., González, N.E., 2010. Holocene vegetation and climate history of central quintana Roo, Yucatán Península, Mexico. Rev. Palaeobot. Palynol. 160, 189–196.

Cheng, H., Fleitmann, D., Edwards, R.L., Wang, X., Cruz, F.W., Auler, A.S., Mangini, A., Wang, Y., Kong, X., Burns, S.J., Matter, A., 2009. Timing and structure of the 8.2 kyr B.P. event inferred from δ18O records of stalagmites from China, Oman, and Brazil. Geology 37, 1007–1010.

Cleef, A.M., 1981. Dissertationes Botanicae. The Vegetation of the Páramos of the Colombian Cordillera Oriental, vol. 71. Cramer, Vaduz, pp. 1–320.

Cleef, A.M., Hooghiemstra, H., 1984. Dissertationes Botanicae. Present Vegetation of the Area Og the High Plain of Bogotá, vol. 79. Cramer, Vaduz, pp. 42–66.

Cleef, A.M., Rangel, J.O., Salamanca, S., Ariza, C.L., Van Reenen, G.B.A., 2005. La vegetación del páramo del Macizo de Tatamá, cordillera Occidental de Colombia. In: Van der Hammen, T., Rangel, J.O., Cleef, A.M. (Eds.), La Cordillera Occidental Colombiana, transecto Tatamá. Estudios de Ecosistemas Tropoandinos, Berlin-Suttgart, vol. 6, pp. 377–468.

Clement, A.C., 1999. Orbital controls on the el Nino/southern oscillation and the tropical climate. Paleoceanography 14, 441–456.

Clement, A.C., Cane, M.A., Seager, R., 2001. An orbitally driven tropical source for abrupt climate change. J. Clim. 14, 2369–2375.

Cook, K.H., 2009. SAn climate variability and change: remote and regional forcing processes. In: Vimeux, F., Sylvestre, F., Khodri, M. (Eds.), Past Climate Variability in SA and Surrounding Regions, from the Last Glacial Maximum to the Holocene. Springer Science + Business Media B.V, pp. 193–211.

Cuatrecasas, J., 1958. Aspectos de la vegetación natural de Colombia. Revista de la Academia Colombiana de Ciencias Exactas. Físicas Nat. 10, 221–264.

Debret, M., Sebag, D., Crosta, X., Massei, N., Petit, J.R., Chapron, E., Bout-Roumazeilles, V., 2009. Evidence from wavelet analysis for a mid-Holocene transition in global climate forcing. Quat. Sci. Rev. 28, 2675–2688.

Espinal, L.S., 1992. Geografía ecológica de Antioquia. Zonas de vida. Universidad Nacional de Colombia, Medellín, 146 pp.

Espinal, S., Boeke, J., McElroy, J., 1983. Notas sobre la flora del páramo de Frontino (Urrao). Gallencia 13, 85–88.

Faegri, K., Iversen, J., 1989. Textbook of Pollen Analysis, fourth ed. Wiley, Chichester. 328 pp.

Farge, M., 1992. Wavelet transforms and their applications to turbulence. Annu. Rev. Fluid Mech. 24, 395–458.

Flantua, S., Hooghiemstra, H., Grimm, E.C., Behling, H., Bush, M.B., González-Arango, C., Gosling, W., Ledru, M.-P., Lozano-García, S., Maldonado, A., Prieto, A., Rull, V., Van Boxel, J.H., 2015. Updated site compilation of the Latin American Pollen Database; challenging new research. Rev. Palaeobot. Palynol. 223, 104–115.

Flantua, S.G.A., Hooghiemstra, H., Vuille, M., Behling, H., Carson, J.F., Gosling, W.D., Hoyos, I., Ledru, M.P., Montoya, E., Mayle, F., Maldonado, A., Rull, V., Tonello, M.S., Whitney, B.S., Gonzalez-Arango, C., 2016a. Climate variability and human impact in SA during the last 2000 years: synthesis and perspectives from pollen records. Clim. Past 12, 483–523.

Flantua, S.G.A., Blaauw, M., Hooghiemstra, H., 2016b. Geochronological database and classification system for age uncertainties in Neotropical pollen records. Clim. Past 12, 387–414.

Fox, J., Andersen, R., 2005. Using the R Statistical Computing Environment to Teach Social Statistics Courses. Department of Sociology, McMaster University, 36 pp.

Fu, R., Dickinson, R.E., Chen, M., Wang, H., 2001. How do tropical sea surface temperatures influence the seasonal distribution of precipitations in the equatorial Amazon. J. Clim. 14, 4003–4026.

Gentry, A.H., 1995. Patterns of diversity and floristic composition in neotropical montane forests. In: Churchill, S.P., Balslev, H., Forero, E., Luteyn, J.L. (Eds.), Biodiversity and Conservation of Neotropical Montane Forests. Proceedings. New York Botanical Garden, pp. 103–126.

González, E., Van der Hammen, T., Plint, R.F., 1965. Late Quaternary vegetational sequence in Valle de Lagunillas, Sierra Nevada del Cocuy. Colomb. Leidse Geol. 32, 157–182.

González-Carranza, Z., Hooghiemstra, H., Vélez, M.I., 2012. Major altitudinal shifts in Andean vegetation on the Amazonian flank show temporarily loss of biota in the Holocene. Holocene 22, 1227–1241.

Grimm, E.C., 1987. CONISS: a FORTRAN 77 program for stratigraphically constrained cluster analysis by the method of incremental sum of squares. Comput. Geosci. 13, 13–35.

Groot, M.H.M., Bogotá, R.G., Lourens, L.J., Hooghiemstra, H., Vriend, M., Berrio, J.C., Tuenter, E., et al., 2011. Ultra-high resolution pollen record from the northern Andes reveals rapid shifts in montane climates within the last two glacial cycles. Clim. Past. 7, 299–316.

Groot, M.H.M., Hooghiemstra, H., Berrio, J.-C., Giraldo, C., 2013. North Andean environmental and climatic change at orbital to submillennial time-scales: vegetation, water-levels, and sedimentary regimes from Lake Fúquene during 130-27 ka. Rev. Palaeobot. Palynol. 197, 186–204.

Hansen, B.C.S., Rodbell, D.T., Seltzer, G.O., León, B., Young, K.R., Abbott, M., 2003. Late-glacial and Holocene vegetational history from two sites in the western Cordillera of southwestern Ecuador. Palaeogeogr. Palaeoclimatol. Palaeoecol. 194, 79–108.

Haug, G.H., Highen, K.A., Sigman, D.M., Peterson, L.C., Röhl, U., 2001. Southward migration of the intertropical convergence zone through the Holocene. Science 293, 1304–1308.

Haug, G.H., Günther, D., Petersen, L.C., Sigman, D.M., Hughen, K.A., Aeschlimann, B., 2003. Climate and the collapse of Maya civilization. Science 299, 1731–1735.

Helmke, J.P., Bauch, H.A., Röhl, U., Mazaud, A., 2005. Changes in sedimentation patterns of the Nordic seas region across the mid-Pleistocene. Mar. Geol. 215, 107–122.

Hernández, A., Giralt, S., Bao, R., Sáez, A., Leng, M.J., Barker, P.A., 2010. ENSO and solar activity signals from oxygen isotopes in diatom silica during late glacial-Holocene transition in Central Andes (18°S). J. Paleolimnol. 44, 413–429.

Hodell, D.A., Anselmetti, F.S., Ariztegui, D., Brenner, M., Curtis, J.H., Gilli, A., Grzesik, D.A., Guilderson, T.J., Müller, A.D., Bush, M.B., Correa-Metrio, A., Escobar, J., Kutterolf, S., 2008. An 85-ka record of climate change in lowland Central America. Quat. Sci. Rev. 27, 1152–1165.

Hooghiemstra, H., 1984. Dissertationas botanicae. Vegetational and Climatic History of the High Plain of Bogotá, Colombia: a Continuous Record of the Last 3.5 Million Years, vol. 79. J. Cramer, Vaduz, 368 pp.

Hooghiemstra, H., 1989. Quaternary and Upper Pliocene glaciations and forest development in the tropical Andes: evidence from a long high-resolution pollen record from the sedimentary basin of Bogotá, Colombia. Palaeogeogr. Palaeoclimatol. Palaeoecol. 72, 11–26.

Hooghiemstra, H., Ran, E.T.H., 1994. Late and Middle Pleistocene climatic change and forest development in Colombia: pollen record Funza II (2-158 m core interval). Palaeogeogr. Palaeoclimatol. Palaeoecol. 109, 211–246.

Hooghiemstra, H., Berrio, J.C., Groot, M.H.M., Bogotá-, A.R.G., Moscol-Olivera, M., González-Carranza, Z., 2012. The dynamic history of the upper forest line ecotone in the northern Andes. In: Randall, R.W. (Ed.), Ecotones between Forest and Grassland. Springer-Science and Business Media, New York, pp. 229–246.

Islebe, G.A., Hooghiemstra, H., Van der Borg, K., 1995. A cooling event during the younger Dryas chron in Costa Rica. Palaeogeogr. Palaeoclimatol. Palaeoecol. 117, 73–80.

Jansen, J.H.F., Van der Gaast, S.J., Koster, B., Vaars, A.J., 1998. CORTEX, a shipboard XRFscanner for element analyzes in split sediment cores. Mar. Geol. 151, 143–153.

Jaramillo, D., Parra, N., 1993. Aspectos biofísicos generales del Páramo de Frontino. Rev. del ICNE 4 (2), 81–96. Colombia.

Kuhry, P., 1988. Dissertationes Botanicae. Palaeobotanical-palaeoecological Studies of Tropical High Andean Peatbog Section (Cordillera Oriental, Colombia), vol. 116. J. Cramer, Berlin-Stuttgart, 241pp.

Labat, D., 2005. Recent advances in wavelet analyzes: part 1. A review of concepts. J. Hydrology 314, 275–288.

Lea, D.W., Pak, D.K., Peterson, L.C., Hughen, K.A., 2003. Synchroneity of tropical and high- latitude Atlantic temperatures over the last glacial termination. Science 301, 1361–1364.

Leyden, B.W., 2002. Pollen evidence for climatic variability and cultural disturbance in the Maya lowlands. Anc. Mesoam. 13, 85–101.

Lozano, G., Parra, L.N., Segecin, R., Ramirez, J.J., 1999. Inferencias paleolimnologicas del Holoceno basadas en diatomeas de la Laguna Puente Largo, Páramo de Frontino, Antioquia. In: Florez, M.T., Lozano, G. (Eds.), Silicofossiles Altoandinos. Ed. Gráficas Montoya, Medellin, Colombia, pp. 57–116.

Marchant, R.A., Behling, H., Berrio, J.C., Cleef, A., Duivenvoorden, J., van Geel, B., van der Hammen, T., Hooghiemstra, H., Kuhry, P., Melief, B.M., van Reenen, G., Wille, M., 2001. Late Holocene Colombian vegetation dynamics. Quat. Sci. Rev. 20, 1289–1308.

Marchant, R.A., Behling, H., Berrio, J.C., Cleef, A., Duivenvoorden, J., van Geel, B., van der Hammen, T., Hooghiemstra, H., Kuhry, P., Melief, B.M., van Reenen, G., Wille, M., 2002. Colombian vegetation derived from pollen data at 0, 3000,

6000, 9000, 12,000, 15,000 and 18,000 radiocarbon year before present. J. Quat. Sci. 17, 113–129.
Marchant, R.A., Berrío, J.C., Behling, H., Boom, A., Hooghiemstra, H., 2006. Colombian dry moist forest transitions in the Llanos Orientales – a comparison of model and pollen-based biome reconstructions. Palaeogeogr. Palaeoclimatol. Palaeoecol. 234 (1), 28–44.
Marchitto, T.M., Muscheler, R., Ortiz, J.D., Carriquiry, J.D., Van Geen, A., 2010. Dynamical response of the tropical Pacific Ocean to solar forcing during the early Holocene. Science 330, 1378–1381.
Mayewski, P.A., Rohling, E.E., Stager, J.C., Karlén, W., Maasch, K.A., Meeker, L.D., Meyerson, E.A., Gasse, F., van Krefeld, S., Holmgren, K., Lee-Thorp, J., Rosqvist, G., Rack, F., Staubwasser, M., Schneider, R.R., Steig, E.J., 2004. Holocene climate variability. Quat. Res. 62, 243–255.
Mommersteeg, H., 1998. Vegetation Development and Cyclic and Abrupt Climatic Change during the Late Quaternary. Ph.D. thesis. University of Amsterdam, Nehterlands, 212 pp.
Monsalve, C., 2015. Climatic Change during the Late Glacial in the Northwestern Part of Colombia, Based on Palynology and Microfluorescence-X. Ph.D. Thesis. In: Terre & Environment 134, Earth and Environmental Science Section. University of Geneva, 149 pp. E-access. http://archive-ouverte.unige.ch/unige:81059.
Moscol Olivera, M., Hooghiemstra, H., 2010. Three millennia upper forest line changes in northern Ecuador : pollen records and altitudinal vegetation distributions. Rev. Palaeobot. Palynol. 163, 113–126.
Moy, C.M., Seltzer, G.O., Rodbell, D.T., Anderson, D.M., 2002. Variability of el Niño/southern oscillation activity at millennial timescales during the Holocene epoch. Nature 420, 162–165.
Muñoz, P., 2013. Holocene Climate Variability in Tropical SA : Case History from a High-mountain Wet Zone in NW Colombia Based on Palynology and X-ray Microfluorescence. Ph. D. Thesis. In: Terre & Environment 124, Earth and Environmental Science Section. University of Geneva, 178 pp. E-access. http://archive-ouverte.unige.ch/unige:34298.
Niemann, H., Haberzettl, T., Behling, H., 2009. Holocene climate variability and vegetation dynamics inferred from the (11700 cal yr BP) Laguna Rabadilla de Vaca sediment record, southeastern Ecuadorian Andes. Holocene 19 (2), 307–316.
Parra, L.N., 1991. Geología glacial del Páramo de Frontino. Universidad Nacional de Colombia, Medellín, 44 pp. (unpubl.).
Parra, L.N., 2005. Análisis facial de alta resolución de sedimentos del Holoceno Tardío en el Páramo de Frontino, Antioquia. Ph.D. Tesis. Instituto de Ciencias Naturales. Universidad Nacional de Colombia, Bogotá, 215 pp. E-access. http://www.bdigital.unal.edu.co/10719/.
Parra, L.N., Jaramillo, A., 1999. In: Montoya, Gráficas (Ed.), Análisis palinológico del núcleo Puente Largo Páramo de Frontino. Medellín, 236 pp.
Parra, L.N., Rangel, O., Van der Hammen, T., 2010a. Geomorfología del Páramo de Frontino. In: Rangel, J.O. (Ed.), Colombia diversidad biótica 10, Instituto de Ciencias Naturales. Universidad Nacional de Colombia, Bogotá, pp. 1–14.
Parra, L.N., Rangel, J.O., Van der Hammen, T., 2010b. Modelo de facies para los humedales paramunos. In: Rangel, J.O. (Ed.), Colombia diversidad biótica 10, Instituto de Ciencias Naturales. Universidad Nacional de Colombia, Bogotá, pp. 15–41.
Parra, L.N., Rangel, J.O., Van der Hammen, T., 2010c. Los sedimentos paramunos y la estratigrafía de la turbera Llano Grande, Páramo de Frontino (Antioquia, Colombia). In: Rangel, J.O. (Ed.), Colombia diversidad biótica 10, Instituto de Ciencias Naturales. Universidad Nacional de Colombia, Bogotá, pp. 67–91.
Parra, L.N., Rangel, J.O., Van der Hammen, T., 2010d. Las tefras de los humedales del Páramo de Frontino (Antioquia, Colombia). In: Rangel, J.O. (Ed.), Colombia diversidad biótica 10, Instituto de Ciencias Naturales. Universidad Nacional de Colombia, Bogotá, pp. 93–100.
Petersen, L.C., Haug, G.H., 2006. Variability in the mean latitude of the Atlantic intertropical convergence zone as recorded by riverine input of sediments to the Cariaco Basin (Venezuela). Palaeogeogr. Palaeoclimatol. Palaeoecol. 234, 97–113.
Petersen, L.C., Haug, G.H., Hughen, K.A., Röhl, U., 2000. Rapid changes in the hydrologic cycle of the tropical Atlantic during the last glacial. Science 290, 1947–1951.
Piperno, D.R., Jones, J.G., 2003. Paleoecological and archaeological implications of a latePleistocene/Early Holocene record of vegetation and climate from the Pacific coastal plain of Panama. Quat. Res. 59, 79–87.
Poveda, G., Mesa, O.J., 2000. On the existence of Lloró (the rainiest locality on Earth): Enhanced ocean-atmosphere-land interaction by a low level jet. Geophys. Res. Lett. 27, 1675–1678.
Poveda, G., Jaramillo, A., Gil, M.M., Quiceno, N., Mantilla, R., 2001. Seasonality in ENSO related precipitation, river discharges, soil moisture, and vegetation index (NDVI) in Colombia. Water Resour. Res. 37, 2169–2178.
Rangel, J.O., 1995. La diversidad florística en el espacio andino de Colombia. In: Churchill, S.P., Balslev, H., Forero, E., Luteyn, J.L. (Eds.), Biodiversity and Conservation of Neotropical Montane Forests. Proceedings. New York Botanical Garden, pp. 187–205.
Rangel, J.O. (Ed.), 2010. Colombia Diversidad Biótica X. Cambio global (natural) y climático (antrópico) en el páramo colombiano. Universidad Nacional de Colombia, Instituto de Ciencias Naturales, Bogotá, 556 pp.
Rangel, J.O., Aguilar, M., 1995. Una aproximación sobre la diversidad climática en las regiones naturales de Colombia. In: Rangel, J.O. (Ed.), Colombia Diversidad Biótica 1, Editorial Guadalupe, Santafe de Bogotá.
Rangel, J.O., Van der Hammen, T., Jaramillo, R., 1982. Tipos de vegetación en el transecto Buritaca-La Cumbre Sierra Nevada de Santa Marta (entre 0 y 4100 m). Colomb. Geográfica 10, 1–18.
Rangel, J.O., Lowy-, C.P., Aguilar, M. (Eds.), 1997. Colombia: Diversidad Biótica II. Tipos de vegetación en Colombia. Instituto de Ciencias Naturales – IDEAM, Santafé de Bogotá, 436 pp.
Rangel, J.O., Sánchez, D., Ariza, C., 1999. Fitosociología del Páramo de Frontino. In: Montoya, Gráficas (Ed.), Tardiglacial y Holoceno del norte de la Cordillera Occidental de Colombia, p. 236. Medellín.
Rasmusen, S.O., Andersen, K.K., Svensson, A.M., Steffensen, J.P., Vinther, B.M., Clausen, H.B., Siggaard-Andersen, M.L., Johnsen, S.J., Larsen, L.B., Dahl-Jensen, D., Bigler, M., Röthlisberger, R., Fischer, H., Goto-Azuma, A., Hansson, M.E., Ruth, U., 2006. A new Greenland ice core chronology for the last Glacial termination. J. Geophys. Res. 111, D06102. http://dx.doi.org/10.1029/2005JD006079.
Reimer, P., Baillie, M., Bard, E., Bayliss, A., Beck, J., Bertrand, C., Backwell, P., Buck, C., Burr, G., Cutler, K., Damon, P., Edwards, R., Fairbanks, R., Friedrich, M., Guilderson, T., Hogg, A., Hughen, K., Kromer, B., McCormac, G., Manning, S., Bronk Ramsey, C., Reimer, R., Remmele, S., Southon, J., Stuiver, M., Talamo, S., Taylor, F., Van der Plicht, J., Weyhenmeyer, C., 2004. IntCal04 terrestrial radiocarbon age calibration, 0–26 cal kyr BP. Radiocarbon 46 (3), 1029–1058.
Renssen, H., Seppä, H., Heiri, O., Roche, D.M., Goosse, H., Fichefet, T., 2009. The spatial and temporal complexity of the Holocene thermal maximum. Nat. Geosci. 2, 411–414.
Renssen, H., Seppä, H., Crosta, X., Goosse, H., Roche, D.M., 2012. Global characterization of the Holocene thermal maximum. Quat. Sci. Rev. 48, 7–19.
Riedinger, M.A., Steinitz-Kannan, M., Last, W.M., Brenner, M., 2002. A 6100 14C yr record of el Niño activity from the Galapagos islands. J. Palaeolimnol 27, 1–7.
Rodbell, D.T., Seltzer, G.O., Anderson, D.M., Abbott, M.B., Enfield, D.B., Newman, J.H., 1999. An ~15,000-year record of El Niño-driven alluviation in southwestern Ecuador. Science 283, 516–520.
Röhl, U., Abrams, L.J., 2000. High-resolution, downhole and nondestructive core measurements from sites 999 and 1001 in the Caribbean sea: application to the late Paleocene thermal maximum. Proc. Ocean. Drill. Prog. Sci. Results 165, 191–203.
Rohling, E.J., Palike, H., 2005. Centennial-scale climate cooling with a sudden cold event around 8200 years ago. Nature 434, 975–979.
Roubik, D.W., Moreno, J.E., 1991. Pollen and Spores of Barro Colorado Island. In: Monographs in Sytematic Botany, vol. 36. Missouri Botanical Garden, 268 pp.
Rull, V., Abbott, M.B., Polissar, P.J., Wolfe, A.P., Bezada, M., Bradley, R.S., 2005. 15'000-yr pollen record of vegetation change in high-altitude tropical Andes at Laguna Verde Alta, Venezuela. Quat. Res. 64, 308–317.
Ryan, P.D., Harper, D.A.T., Whalley, J.S., 1995. PALSTAT, Statistics for Palaeontologists. Chapman and Hall (now Kluwer Academic Publishers), 31 pp.
Salomons, J.B., 1986. Paleoecology of volcanic soils in the Colombian Central Cordillera (Parque Nacional Natural de Los Nevados). Ph.D. thesis. University of Amsterdam, Netherlands. The Quaternary of Colombia, p. 13.
Sánchez, D., 1998. Inventario florístico del páramo de Frontino (Urrao) Antioquia. Rev. Fac. Nac. Agron. 51 (2), 99–156.
Stansell, N.D., Abbott, M.B., Rull, V., Rodbell, D.T., Bezada, M., Montoya, E., 2010. Abrupt Younger Dryas cooling in the northern tropics recorded in lake sediments from the Venezuelan Andes. Earth Planet. Sci. Lett. 293, 154–163.
Stott, L., Poulsen, C., Lund, S., Thunell, R., 2002. Super ENSO and global climate oscillations at millennial time scales. Science 297, 222–226.
Stuiver, M., Reimer, P.J., 1993. Extended 14C data base and revised CALIB 3.0 14C age calibration program. Radiocarbon 2, 215–230.
Talma, A.S., Vogel, J.C., 1993. A simplified approach to calibrating 14C dates. Radiocarbon 2, 317–322.
Thompson, L.G., 2000. Ice core evidence for climate change in the Tropics: implications for our future. Quat. Sci. Rev. 19, 19–35.
Thompson, L.G., Mosley-Thompson, E., Davis, M.E., Lin, P.N., Henderson, K.A., Cole-Dai, J., Bolzan, J.F., Liu, K.B., 1995. Late Glacial stage and Holocene tropical ice core records from Huascarán. Peru. Sci. 269, 46–50.
Thompson, L.G., Mosley-Thompson, E., Henderson, K.A., 2000. Ice-core palaeoclimate records in tropical SA since the last glacial maximum. J. Quat. Sci. 15 (4), 377–394.
Thouret, J.C., Cantagrel, J.M., Robin, C., Murcia, C., Salinas, R., Cepeda, H., 1995. Quaternary eruptive history and hazard-zone model at Nevado del Tolima and Cerro Machin volcanoes, Colombia. J. Volcanol. Geotherm. Res. 66, 397–426.
Thouret, J.C., Van der Hammen, T., Salomon, B., Juvigné, E., 1996. Paleoenvironmental changes and glacial stades of the last 50'000 years in the Cordillera Central, Colombia. Quat. Res. 46, 1–18.
Torrence, C., Compo, G., 1998. A practical guide to wavelet analysis. Bull. Amer. Meteorol. Soc. 79 (1), 61–78.
Torres, V., 2005. Pliocene-pleistocene Evolution of Flora, Vegetation and Climate: a Palynological and Sedimentological Study of a 586 M Core from the Bogotá Basin, Colombia. Ph D Thesis. Institute for Biodiversity and Ecosytems Dynamic (IBED), University of Amsterdam, 181 pp.
Torres, V., Vandenberghe, J., Hooghiemstra, H., 2005. An environmental reconstruction of the sediment infill of the Bogotá basin (Colombia) during the last 3 million years from abiotic and biotic proxies. Palaeogeogr. Palaeoclimatol. Palaeoecol. 226, 127–148.
Torres, V., Hooghiemstra, H., Lourens, L., Tzedakis, P.C., 2013. Astronomical tuning of long pollen records reveals the dynamic history of montane biomes and lake levels in the tropical high Andes during the Quaternary. Quat. Sci. Rev. 63,

59–72.
Urrego, D.H., Hooghiemstra, H., Rama-Corredor, O., Martrat, B., Grimalt, J.O., Thompson, L., Bush, M.B., González-Carranza, Z., Hanselman, J., Valencia, B., Velásquez-Ruiz, C., 2016. Millennial-scale vegetation changes in the tropical Andes using ecological grouping and ordination methods. Clim. Past 12, 697–711.
Van Boxel, J.H., González-Carranza, Z., Hooghiemstra, H., Bierkens, M., Vélez, M.I., 2014. Reconstructing past precipitation from lake levels and inverse modelling for Andean lake La Cocha. J. Palaeolimnol. 51, 63–77.
Van der Hammen, T., 1974. The Pleistocene change of vegetation and climate in tropical SA. J. Biogeogr. 1, 3–26.
Van der Hammen, T., González, E., 1960a. Holocene and late glacial climate and vegetation of páramo Palacio (eastern cordillera, Colombia, SA). Geol. Mijnb. 39 (12), 737–746.
Van der Hammen, T., González, E., 1960b. Upper Pleistocene and Holocene climate vegetation of the "Sabana de Bogotá", (Colombia, SA). Leidse Geol. Meded. 25, 126–315.
Van der Hammen, T., González, E., 1963. Historia de clima y vegetación del Pleistoceno Superior y del Holoceno de la Sabana de Bogotá. Bol. Geol. (XI) 1–3, 189–266.
Van der Hammen, T., Hooghiemstra, H., 1995. The el Abra stadial, a younger Dryas equivalent in Colombia. Quat. Sci. Rev. 14, 841–851.
Van der Hammen, T., Hooghiemstra, H., 2003. Interglacial-glacial Fúquene-3 pollen record from Colombia: an Eemian to Holocene climate record. Glob. Planet. Change 36, 181–199.
Van der Hammen, T., Werner, J.H., Van Dommelen, H., 1973. Palynological record of the northern Andes: a study of the Pliocene and lower quaternary of the Colombian eastern cordillera and the early evolution of its high-Andean biota. Rev. Palaeobot. Palynol. 16, 1–122.
Van der Hammen, T., Barelds, J., De Jong, H., De Veer, A.A., 1980/1981. Glacial sequence and environmental history in the Sierra Nevada del Cocuy (Colombia). Palaeogeogr. Palaeoclim. Palaeoecol. 32, 247–340.
Van der Hammen, T., Rangel, O., Cleef, A.M. (Eds.), 2005. La Cordillera Occidental Colombiana Transecto Tatamá. Studies on Colombian Ecosystems 6, Cramer-borntraeger, Berlin-Stuttgart, 972 pp.
Van Geel, B., Van der Hammen, T., 1973. Upper Quaternary vegetational and climatic sequence of the Fúquene area, Eastern Cordillera, Colombia. Palaeogeogr. Palaeoclim. Palaeoecol. 14, 9–92.
Van 't Veer, R., Hooghiemstra, H., 2000. Montane forest evolution during the last 650 000 yr in Colombia: a multivariate approach based on pollen record Funza-I. J. Quat. Sci. 15, 329–346.
Van 't Veer, R., Islebe, G.A., Hooghiemstra, H., 2000. Climatic change during the younger Dryas chron in Northern SA: a test of the evidence. Quat. Sci. Rev. 19, 1821–1835.
Velásquez, C.A., 1999. Análisis palinológico del núcleo Llano Grande Páramo de Frontino. In: Montoya, Gráficas (Ed.), Tardiglacial y Holoceno del norte de la Cordillera Occidental de Colombia. Medellín, 236 pp.
Velásquez, C.A., 2005. Paleoecologia de alta resolucion del Holoceno Tardio en el Páramo de Frontino, Antioquia, Colombia. Quat. Colombia 30, 199 pp. E-access. http://www.bdigital.unal.edu.co/12363/.
Velásquez, C.A., Hooghiemstra, H., 2013. Pollen-based 17-kyr forest dynamics and climate change from the Western Cordillera of Colombia; no-analogue associations and temporarily lost biomes. Rev. Paleobot. Palynol. 194, 38–49.
Velásquez, C.A., Parra, L.N., Sanchez, C., Rangel, J.O., Ariza, C.L., Jaramillo, A., 1999. In: Montoya, Gráficas (Ed.), Tardiglacial y Holoceno del norte de la Cordillera Occidental de Colombia. Medellin, Colombia, 236 pp.
Vélez, M.I., Wille, M., Hoohiemstra, H., Metcalfe, S., Vandenberghe, J., Van der Borg, K., 2001. Late Holocene environment history of southern Chocó region, Pacific Colombia; sediment, diatom and pollen analysis of core El Caimito. Palaeogeogr. Palaeoclim. Palaeoecol. 173, 197–214.
Vélez, M.I., Hooghiemstra, H., Metcalfe, S., Wille, M., Berrío, J.C., 2006. Late Glacial and Holocene environmental and climatic changes from a limnological transeat through Colombia, Northern SA. Palaeogeogr. Palaeoclim. Palaeoecol. 234, 81–96.
Vizy, E.K., Cook, K.H., 2007. Relationship between Amazon and high Andes rainfall. J. Geophys. Res. 112, D07107.
Vuille, M., Garreaud, R.D., 2012. Ocean-atmosphere interactions on interannual to decadal timescales. In: Matthews, J.A., Bartlein, K.R., Briffa, A., Dawson, A., de Vernal, A., Denham, T., Fritz, S.C., Oldfield, F. (Eds.), Handbook of Environmental Change, vol. 1. Sage Publications, London, Los Angeles, New Delhi, Singapore, pp. 471–496.
Vuille, M., Werner, M., 2005. Stable isotopes in precipitation recording South American summer monsoon and ENSO variability – observations and model results. Clim. Dynam 25, 401–413.
Wanner, H., Beer, J., Bütikofer, J., Crowley, T.J., Cubasch, U., Flückiger, J., Goosse, H., Grosjean, M., Joos, F., Kaplan, J.O., Küttel, M., Müller, S.A., Prentice, I.C., Solomina, O., Stocker, T.F., Tarasov, P., Wagner, M., Widmann, M., 2008. Mid- to late Holocene climate change: an overview. Quat. Sci. Rev. 27, 1791–1828.
Wanner, H., Mercolli, L., Grosjean, M., Ritz, S.P., 2014. Holocene climate variability and change; a data-based review. J. Geol. Soc. Lond. http://dx.doi.org/10.1144/jgs2013-101.
Waylen, P., Poveda, G., 2002. El Niño–southern oscillation and aspects of western SAn hydro-climatology. Hydrol. Process. 16, 1247–1260.
Weng, H., Lau, K.M., 1994. Wavelets, period doubling, and time-frequency localization with application to organization of convection over the tropical western Pacific. J. Atmos. Sci. 51, 2523–2541.
Weng, C., Bush, M.B., Curtis, J.H., Kolata, A.L., Dillehay, T.D., Binford, M.W., 2006. Deglaciation and Holocene climate change in the western Peruvian Andes. Quat. Res. 66, 87–96.
Wille, M., Hooghiemstra, H., Behling, H., Van der Borg, K., Negret, A.J., 2001. Environmental change in the Colombian subandean forest belt from 8 pollen records: the last 50 kyr. Veg. Archaeobotany 10, 61–77.
Wille, M., Hooghiemstra, H., van Geel, B., Behling, H., de Jong, A., van der Borg, K., 2003. Submillennium-scale migrations of the rainforest-savanna boundary in Colombia: 14C wigglematching and pollen analysis of core Las Margaritas. Palaeogeogr. Palaeoclimatol.,Palaeoecol. 193, 201–223.
Yancheva, G., Nowaczyk, N.R., Mingram, J., Dulski, P., Schettler, G., Negendank, J.F.W., Liu, J., Sigman, D.M., Peterson, L.C., Haug, G.H., 2007. Influence of the intertropical convergence zone on the East Asian monsoon. Nature 445, 74–77.
Yi, H., Shu, H., 2012. The improvement of the Morlet wavelet for multi-period analysis of climate data. C.R. Geosci. 344, 483–497.